Distributed Cooperative Control and Optimization of Connected Automated Vehicles Platoon Against Cut-in Behaviors of Social Drivers

Bohui Wang, *Senior Member, IEEE,* **Rong Su,** *Senior Member, IEEE* *

September 1, 2022

*B. Wang and R. Su are with the Department of Electrical and Electronic Engineering, Nanyang Technological University, Singapore 639798 (e-mail: bhwang@ntu.edu.sg; rsu@ntu.edu.sg)

ABSTRACT

Connected automated vehicles (CAVs) have brought new opportunities to improve traffic throughput and reduce energy consumption. However, the uncertain lane-change behaviors (LCBs) of surrounding vehicles (SVs) as an uncontrollable factor significantly threaten the driving safety and the consistent movement of a group of platoon CAVs. How to ensure safe, efficient, and fuel economic platoon control poses a key challenge faced by researchers in complex traffic environments. This study proposes a dynamic platoon management and cooperative driving framework for a mixed traffic flow consisting of multiple CAVs and possible human-driven vehicles (HDVs) as the SVs on unsignalized roads. In the proposed framework, the leader CAV of the platoon provides a high-level automatic driving decision to the follower CAVs by developing an optimal trajectory estimation of the HDVs while distributed observers and tracking controllers are properly implemented by the follower CAVs. Specifically, the proposed framework consists of three stages. At the observation stage, the cruising information of all the SVs will be collected by the leader CAV through the Cellular-Vehicle-to-X (C-V2X) infrastructure, while an automatic decision-making driving assistance system (ADMDSS) is constructed to determine the driving states of the platoon. When the HDVs approach the communication range of the platoon, in the prediction stage, the trajectories of the HDVs as the target vehicles will be estimated and the reference trajectory planning for the leader CAV and the cooperative controller design for the follower CAVs will be respectively activated by using C-V2X infrastructure. More importantly, we consider two types of social driving behaviors (SDBs): courteous and rude, where the optimal trajectory estimation will be obtained based on the known social preferences of the SVs. While the HDVs deliver their social cut-in intentions (SCIIs) into the platoon CAVs, the ADMDSS will provide a high-level trajectory guidance to the platoon CAVs to adjust the time-varying space error among the CAVs while the problems of collision avoidance and energy composition will be solved at the lane change stage within a finite time by proposing a cooperative trajectory tracking optimization algorithm. Simulation cases are presented to illustrate the effectiveness of the proposed approaches.

***Index Terms*—Connected automated vehicles (CAVs); cooperative driving; dynamic platoon management; social cut-in behaviors; optimization; distributed control; car-following model; formation control.**

I. Introduction

TODAY, intelligence and mobility have been regarded as important factors to measure the effectiveness of smart cities, where efficient vehicle control and safe cruising are imposing two major challenges for intelligent traffic management. Importantly, as an economical and green way to improve traffic conditions, connected automated vehicles (CAVs) can offer better driving quality and safety levels, especially for aging drivers [1], [2]. With the advancement of Cellular-Vehicle-to-X (C-V2X) techniques, the CAVs can sense changes in the surrounding vehicles (SVs) and traffic environment faster and more accurately, which will construct a heterogeneous and mixed transportation system where all the SVs could be interconnected with each other. Although the connectivity can provide precise knowledge of the traffic flow cruising on the entire road network and help achieve the goal of optimizing traffic flow and reducing congestion, the realization of this goal is often restricted by human-driven vehicles (HDVs) as uncontrollable surrounding environments, and one typical example is the sudden lane-change behaviors (LCBs) that are very generally on the road. As reported by the U.S. Department of Transportation, 240,000 to 610,000 annual crashes are related to LCBs [3]. Specifically, cut-in behaviors (CIBs) as a kind of LCBs, aiming to move into the adjacent space ahead of closely followed vehicles in the neighboring lanes, are potentially dangerous and may lead to traffic congestion and increase the risk of accidents [4]. Notably, most CIBs are premeditated, such as drivers planning their trajectories to get better driving priorities, which imposes a challenge for platoon control designers to develop a safe and effective control framework to coordinate the platoon efficiency and driving safety and reduce the influence of CIBs of the HDVs.

Controlling a platoon to optimize energy consumption and improve safety has been studied extensively over the past few years. The early adaptive cruise control (ACC) [5] is to handle the information interaction to enhance driving safety only by standard onboard sensors. Then, cooperative adaptive cruise control (CACC) [6] aims to create a smaller headway distance among CAVs by employing wireless communication and radar measurements. After that, the bidirectional interaction topology policy [7] and the vehicle look-ahead topology policy [8] were proposed to obtain a more flexible design for the platoon model. With the help of consensus theory, the cooperative platoon control framework has been recently developed [9]–[12], which tends to design flexible communication topology and control protocol to improve the practicability. Notably, although ACC and CACC provide a basic control form of CAVs, they all rely on a fixed communication pattern; Cooperative platoon control can schedule communication resources, but they both are linearized models which cannot fundamentally reflect the nonlinear relationship between actual driving behaviors and external stimuli. A car-following model, as a nonlinear model, called "Optimal Velocity Model" (OVM) [13]–[15], can describe how one driver responds to a single stimulus from other vehicles, in which the following behaviors of individual vehicles and the perception mechanism of drivers are two important factors of describing traffic models. Although these studies are very helpful in understanding the driving behaviors of CAVs, it only takes the driver's response into account to a single stimulus without considering cooperative behaviors, while multiple surrounding stimuli and the driver's driving sensitivity will affect the platoon control safety. Recently, an integrated approach was proposed in [16] that takes full advantage of consensus theory to cooperatively deal with multiple peripheral stimuli for purse CAVs but it cannot be applied to mixed traffic situations where HDVs exist. Notably, CAVs and HDVs will coexist on roads, creating a competitive and mixed traffic environment, in which the platoon CAVs would inevitably encounter the LCBs by the HDVs in adjacent lanes, which brings a big challenge for platoon management of CAVs.

In general, there are two classes of methods addressing the platoon control for mixed traffic flows to ensure driving safety and increase traffic throughput. The first one focuses on platoon maneuvers for mixed traffic vehicles to benefit the ambient traffic. For example, the cut-in/cut-out maneuvers under a resilient communication pattern were studied in [17], which only considers the influence of cut-in/cut-out for the last vehicle as an HDV. A hierarchical and implementation-ready cooperative driving framework with mixed traffic flows was developed in [18], where a state transition diagram was designed for different modes of CAVs. A distributed control framework for mixed urban and freeway traffic networks was developed in [19], in which the mixed traffic network is divided among urban agents and freeway agents and each agent solves its optimization problem independently with local information and transmitted information to seek the Nash equilibrium. Furthermore, a mixed traffic flow in which some cars are under car-following control and others are under bilateral control was explored in [20], which provides a necessary stability condition for the mixed traffic flow. Notably, improving the maneuvers for a group of CAVs may cause a larger platoon gap to ensure driving safety but it may also provide a lane-change chance for HDVs to deliver their cut-in intentions (CIIs). Therefore, the second method is to address the LCBs in mixed traffic flows to avoid a collision. For example, a lane-change strategy considering the leading CAV by synthesizing the vehicle velocity prediction, motion planning, and trajectory tracking control was proposed in [21], in which a motion planner is developed to generate the optimal trajectory for a single CAV to implement the lane-change maneuvers; however, the interactions between multiple CAVs and HDVs are missing and the trajectory of HDV is assumed to be certain. A personalized approach of trajectory planning and control based on user preferences was developed in [22] for lane-change of autonomous vehicles, in which all the trajectory candidates are generated by an improved Rapidly-exploring Random Trees that are uncertain. Although the above works involve LCBs, very few studies address how to respond to the LCBs of HDVs. Recently, a deep reinforcement learning-based proactive longitudinal control for CAVs was proposed in [23] to counteract disruptive the LCBs of the HDVs; However, the real vehicle dynamics are ignored by only using the acceleration information and the feasibility of the proposed method depends on the learning accuracy and real-time capability. Notably, HDVs are usually uncontrollable due to the complex CIIs, which makes it difficult for a group of CAVs to maintain the desired platoon performance. In addition, the ultimate efficiency of the platoon is bounded by many uncontrolled factors, i.e., driving sensitivities, social cut-in behaviors (SCIBs), and roads conditions, in which the SCIBs of the HDVs will significantly affect the fuel efficiency of the platoon management of CAVs. Generally, the maximum fuel economy is achieved when vehicles drive at a constant cruising velocity [24]. However, the SCIBs of the HDVs may interrupt the constant movement of the platoon from time to time, making it important to derive a solution that requires a specific platoon management to prevent the SCIBs of the HDVs while maintaining the platoon performance and ensuring safety. Although social driving behaviors (SDBs) for a single HDV have been developed in [25] based on the social preferences of SVs, to the best of our knowledge, there have been no directed reports on the dynamic platoon management and cooperative driving with the rejection of the SCIBs of the HDVs. Therefore, it is necessary to explore the interaction between CAVs and SCIBs of the HDVs to analyze how the HDVs affect the smooth moving performance of platoon CAVs in mixed traffic flows to mitigate traffic congestion and enhance safety.

The aim of this paper is to propose a dynamic platoon management and cooperative driving framework for mixed traffic flows to prevent possible SCIBs of the HDVs while ensuring platoon safety and effectiveness. To this end, we first consider that all the CIBs can be classified into two groups of being rude and being courteous, respectively, due to the fact that humans prioritize social interactions over their own goals when making driving decisions, and then make interpretable decisions to prevent the CIIs of HDVs. Our contributions to this paper are four-fold. Firstly, an integrated trajectory generation and estimation method is proposed to observe and estimate the trajectories of HDVs implemented by the platoon CAVs. Compared with the traditional geometrical approach [26], the dynamic approach [27], and the learning-based approach [28], the influence of SDBs on the trajectory generation and estimation is firstly investigated. Specifically, we shall optimize the estimated trajectory of HDVs by using a parameterized social cost function and the collision check condition. Secondly, the fundamental definition of critical moments in CIBs and an automatic decision-making driving assistance system (ADMDSS) are proposed, where a finite state machine is designed to determine the driving states of the platoon at the observer and prediction stages and then the reference trajectory planning for the leader CAV is designed according to the estimated lane change trajectories of the HDVs and the defined safe buffer field (SBF). Different from the risk assessment method [29], the Stackelberg game method [30], and the intelligent decision-making-based learning strategy [31] that all are only for one leader vehicle, one target vehicle, and one leg vehicle, we formulate an automatic driving decision strategy by considering the longitudinal and lateral positions for a platoon with multiple CAVs and the interaction of SDBs of the HDVs, which is more consistent with actual traffic conditions. Thirdly, we develop a velocity-dependent nonlinear cooperative car-following mode for a group of CAVs to simulate the realistic driving decision while increasing traffic throughput and reducing energy consumption. Compared with the traditional ACC [5], CACC control [6] and cooperative platoon control [9]–[12], we employ cooperative perception, distributed observers, cooperative information interaction, and difference velocity models to dynamically adjust the platoon gap to improve the dynamic platoon performance and reduce the energy consumption and the influence of uncertain SDBs. Lastly, unlike existing works using

ACC-based car-following models in an infinite horizon [32]–[34], the driving safety and fuel efficiency of a fleet of CAVs with a reaction time delay in our work are specifically addressed by designing a cooperative trajectory tracking optimization algorithm to ensure the dynamic platoon to be formed in a finite time. The proposed framework involves trajectory estimation of SDBs of HDVs, driving state determining of the platoon, reference trajectory generation of the leader CAV, and finite-time dynamic platoon formulation to prevent SCIBs of HDVs, which is more promising in mixed traffic flows.

This paper is organized as follows. Section II introduces the problem formulation and driver models. Section III provides the trajectory estimation and optimization for the SCIBs of the HDVs. Section IV proposes a finite-state machine model to describe the platoon management strategy. Section V presents a solution to the finite-time dynamic platoon control and optimization problems. Section VI illuminates the effectiveness of the proposed control framework with simulations. Finally, conclusions and discussions are given in Section VII.

II. Problem Formulation

We consider a cooperative driving, optimization, and automatic decision-making framework as illustrated in Fig. 1. The HDVs are driven by individuals with different driving experiences, while the CAVs travel with a specific cooperative driving technique feasible within a suitable C-V2X infrastructure. The goal is to develop the ADMDSS to efficiently manage the platoon to prevent the SCIBs of the HDVs and ensure cruising safety. In the following, the system formulation and driving model will be given, respectively.

A. Systems formulation

Unlike existing techniques for platoon formulation which only consider a predesigned and fixed inter-space safe distance, the dynamic platoon control and optimization in this framework will consider a complex traffic environment involving a time-varying inter-space policy and the uncontrollable SCIBs of the HDVs and aim to develop a finite-time platoon management strategy to maintain a maximum external-space safe distance between the CAVs and HDVs while having a greater velocity to improve the throughput. To this end, two problems will be addressed, namely $i)$ how to determine the travel conditions and the parameters of control inputs for the CAVs in a mixed car-following environment to ensure safe cruising, and $ii)$ how to efficiently manage the platoon by using an online design of platoon gap to prevent the SCIBs while improving the platoon performance in a finite time?

To formulate the above two problems in Fig. 1, the following statements and constraints are considered:

Statement 1 (Driving modes): **1-1** There are two driving modes for the HDVs containing the *Lane-keeping* and *Lane-change*, and three for the CAVs include the *Cruising*, *Following control*, and *Platoon control*; and **1-2** The HDVs are moving on the *Cruising-lane* and the platoon of CAVs is traveling on the *Target-lane*.

Statement 2 (Vehicle parameters): **2-1** The vehicle parameters for the CAVs and the HDVs are identical; **2-2** The position,

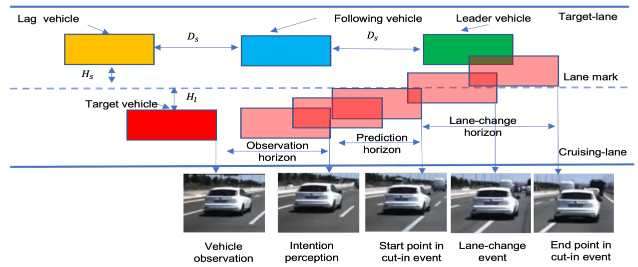

Fig. 1. The arrangement of a platoon in car-following and cut-in environments.

velocity, and acceleration of all the SVs can be measured and observed by using C-V2X infrastructure; and **2-3** The CAVs have a fixed communication range R making the number of HDVs to be considered for SCIBs finite.

Statement 3 (Mixed traffic flows): The platoon contains one *Leader CAV*, one *Lag CAV*, and some *Follower CAVs*. The *Leader CAV* will make the driving decision and the reference trajectory planning. The *Follower CAVs* will drive by their observer information from the *Leader CAV* and their cooperative controllers. The *Lag CAV* is the last *Follower CAVs* whose traveling trajectory will be affected by the platoon size and the position of the HDVs.

Statement 4 (Vehicle roles): All the HDVs of SVs that may interact closely with the platoon CAVs can be divided into the *Front-vehicles*, *Rear-vehicles*, and *Target-vehicles* according to the relative travel distance with respect to the platoon CAVs. The *Front-vehicles* and *Rear-vehicles* keep away from the platoon CAVs, and the *Target vehicles* may interact with the platoon to make CIBs.

Statement 5 (Cut-in procedures): The cut-in procedure contains three stages: *observation stage*, *prediction stage*, and *lane-change stage*. In the *observation stage*, all the CAVs observe the SVs to estimate the trajectory of HDVs. In the *prediction stage*, the *Leader CAV* generates the perception information such as CIIs, velocity, and displacement by using C-V2X infrastructure. In the *lane-change stage*, the HDVs may implement the decision of CIBs.

Statement 6 (Space policies): There are two different types of distances under consideration: a smaller inter-space distance D_s and a larger external-space distance D_c. D_s is a desired safe distance between two consecutive CAVs in the platoon which will be dynamically designed to prevent the CIBs of the *Target vehicles*, and D_c is the traveled distance between the platoon CAVs and the HDVs which will be constructed by a function associated with the lateral and longitudinal of distance and velocity for the SVs.

Constraint 1 (Cruising constraints): The velocity and the acceleration of all the vehicles are bounded by the following constraints

$$v_{min} \leq v_i(t) \leq v_{max}, \tag{1}$$
$$a_{min} \leq a_i(t) \leq a_{max}, \tag{2}$$
$$v_{min} \leq v_{t_i}(t) \leq v_{t_i,max}, \tag{3}$$
$$a_{min} \leq a_{t_i}(t) \leq a_{max}, \tag{4}$$

where v_{min}, $v_{t_i,max}$ and v_{max} are the minimum and maximum speed limits, and a_{min} and a_{max} are the minimum and maximum acceleration for all vehicles, $v_i(t), v_{t_i}(t)$ and $a_i(t), a_{t_i}(t)$ are the velocities and accelerations of the CAV i and the *Target vehicle* t_i, respectively. The considered velocity limit in (1) is smaller than that in (3) to ensure driving safety in a mixed traffic environment.

The basic idea of the proposed framework is to design the ADMDSS which contains a finite state machine to determine the cooperative driving states of the platoon CAVs and a reference trajectory planning for the *Leader CAV*. To this end, it is assumed that the CIIs of HDVs can be detected in the *observation stage* by using the learning method [21], [23]. To ensure driving safety and prevent the CIBs of the HDVs, the platoon CAVs will yield to the possible priorities of the HDVs by using the finite state machine to switch to proper modes, where the *Leader CAV* plays a key role to merge all the observations for the SVs to implement the driving state determination and dynamic platoon management decision. Since the HDVs are uncontrollable, the trajectories of the HDVs will be predicted by the platoon CAVs endowing the estimation of SDBs, while the developed collision check condition will be a constraint to generating the underlying traveling trajectory of CIIs. Under such predicted trajectories, the reference trajectory planning will be designed to provide the desired control input for the *Leader CAV* to prevent all underlying CIBs of the HDVs. By developing a distributed control and optimization strategy, the platoon CAVs will track the reference trajectory planning and follow the ADMDSS to reduce the influence of the SDBs on the HDVs within a finite time.

B. Cooperative driving model

Since the dynamics of platoon CAVs are inherently nonlinear, including the engine, brake system, aerodynamics drag, rolling resistance, gravitational force, etc. [35], we introduce first-order longitudinal dynamics of the acceleration of CAVs to describe the reaction-time delay response of the changes of dynamics of preceding CAVs. Consider a platoon with a group of follower CAVs indexed by $i \in \mathbb{F}$, where $\mathbb{F}$ is an index set. The acceleration dynamics of the i-th CAV can be given by

$$\tau \dot{a}_i(t) + a_i(t) = u_i(t) + y_i(t) + g_i(t), i \in \mathbb{F}, \tag{5}$$

where τ is the delay of the CAV i, $u_i(t)$ is the cooperative control input, and $y_i(t)$ is a car-following model which represents the optimal speed for CAVs with an adjustable sensitivity, and $g_i(t)$ is a difference velocity model which reflects the difference error between the current CAV i and its neighboring CAVs. The vehicle communication can be described by graph theory. Please see [9]–[12] for more details.

Define $s_i(t)$ and $v_i(t)$ as the position and velocity for the CAV i, respectively. Then, the following third-order model is proposed to represent the dynamics of the *Follower CAVs*

$$\begin{aligned} \dot{s}_i(t) =& v_i(t), \\ \dot{v}_i(t) =& a_i(t), \\ \tau \dot{a}_i(t) + a_i(t) =& u_i(t) + y_i(t) + g_i(t), i \in \mathbb{F}. \end{aligned} \tag{6}$$

This paper aims to study how distributed control and optimization methods can ensure efficient platoon management to prevent CIBs of the HDVs under different SDBs. So, it requires that the dynamics of the *Leader CAV* can be programmable based on the perception information and predicted trajectory of HDVs. To this end, the following dynamics of the *Leader CAV* are proposed

$$\begin{aligned} \dot{s}_0(t) =& v_0(t), \\ \dot{v}_0(t) =& a_0(t), \\ \tau \dot{a}_0(t) + a_0(t) =& f(F(t), u_0(t)), \end{aligned} \tag{7}$$

where $s_0(t)$, $v_0(t)$ and $a_0(t)$ are the position, velocity, and acceleration for the *Leader CAV* 0, respectively, $f(F(t), u_0(t))$ is a nonlinear regular function including a finite state machine function $F(t)$ and a planning demand $u_0(t)$ which represents the braking or driving dynamics of the *Leader CAV* to describe the emergent acceleration, deceleration or constant speed to respond the CIIs of the HDVs.

Remark 1: Notably, $F(t)$ is a decision function that is based on the observation and prediction information to determine the cooperative driving states of the platoon under the ADMDSS. Then, the planning demand $u_0(t)$ will be designed to dynamically adjust the platoon gap to prevent the underlying CIBs of the HDVs. Notably, to simplify the analysis, the lateral dynamics of the CAVs will be formulated in this paper using the same longitudinal dynamics according to [36].

III. Trajectories estimation with social driving behaviors under cut-in scenarios

In a congested urban traffic scenario, the gaps between two consecutive CAVs are small. Therefore, the HDVs usually need to actively create a large enough gap by delivering the CIIs to their SVs. However, the SDBs will affect the trajectory planning of HDVs. In what follows, we will introduce the critical moments of SCIBs, the classification of SCIBs, and the trajectory generation methods to formulate the problem of trajectories estimations.

A. Definitions for SCIBs

In order to analyze the dynamic interaction between the platoon CAVs and the HDVs over the whole cut-in process, the following six critical moments (as shown in Fig. 2) are firstly defined:

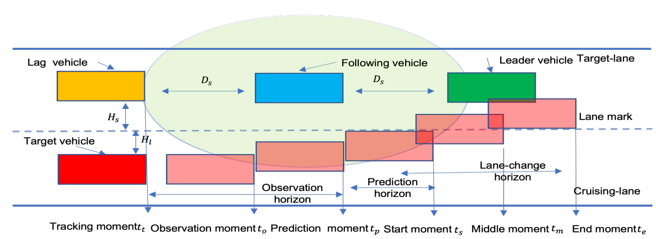

Fig. 2. Critical moments in cut-in behaviors.

Definition 1 (Tracking moment): Let t_t be the *Tracking moment* when the left front tire of the *Target vehicle* enters the communication range R of the platoon CAVs on the *Target-lane*.

Definition 2 (Observation moment): Let t_o be the *Observation moment* when the left front tire of the *Target vehicle* approaches the rear bumper of the platoon CAVs on the *Target-lane*.

Definition 3 (Prediction moment): Let t_p be the *Prediction moment* when the lateral distance of the *Target vehicle to the lane mark is short enough to deliver the CIIs.*

Definition 4 (Start moment): Let t_s be the *Start moment* that refers to the start point of the CIBs in the *prediction stage*, when the left front tire of the *Target vehicle* crosses the lane mark between the *Cruising-lane* and the *Target lane*.

Definition 5 (Middle moment): Let t_m be the *Middle moment* when the centre line of the *Target vehicle* crosses the lane mark during the CIBs.

Definition 6 (End moment): Let t_e be the *End moment* that refers to the end point of the *lane-change stage*, when the *Target vehicle* has finished the CIBs.

Although there exist many SVs in congested traffic, the purpose of this paper is to prevent the underlying CIBs from happening in the middle of the platoon by developing the reference trajectory planning for the *Leader CAV* to adjust the time-varying inter-space policy among the *Follower CAVs* such that only the *Leader CAV* and the *Lag CAV* have strong interactions with the HDVs on the *Target lane*, as shown in Fig. 3, in which social preferences, e.g., rude and courteous SDBs of the HDVs, will be specifically considered in the platoon control and driving state decision. In the following, two types of SCIBs are respectively defined:

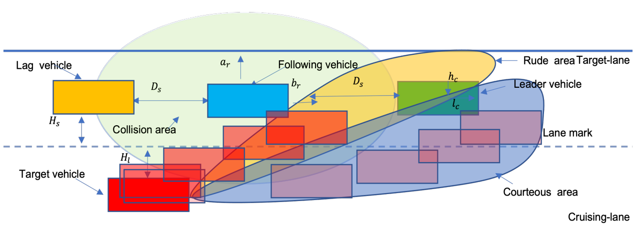

Fig. 3. Social driver cut-in behaviors.

Definition 7 (Rude SCIBs): The HDVs behave rudely and compete for the right of way with the platoon. Aggressive or near-collision behaviors will show in this process and the HDVs traveling at a high speed compete with the platoon CAVs for certain positions in the lane.

Definition 8 (Courteous SCIBs): The HDVs behave courteously and give way to the platoon. Aggressive or near-collision behaviors will not occur during this process and the HDVs travel at a low speed with respect to the platoon.

Remark 2: The definition of six critical moments can depict almost all LCBs and CIBs in the mixed traffic environment when the HDVs travel at a high speed and approaches the platoon CAVs. However, the *Prediction moment* and *Start moment* could happen at the same time. For example, the rude HDVs will change the lateral displacement when approaching the platoon CAVs to get the right of way and deliver their CIIs faster.

Remark 3: Under such two SCIBs, we would like to consider that the platoon shall decelerate to adjust the safe inter-space distance to avoid in advance with respect to the possible rude HDVs or accelerate to surpass the likely courteous HDVs, which will lead to the challenging problems of the trajectory estimation and optimization for the underlying SCIBs of HDVs, the automatic driving decision, the reference trajectory planning for the *Leader CAV*, and the dynamic platoon management of CAVs in a finite time.

B. Trajectories estimation of HDVs with social cost functions

Since all the CAVs can observe the state of the SVs, it is assumed that the intention perception can be known for the platoon CAVs so that the *Leader CAV* can predict the CIIs of the HDVs. It is considered that the start points and end points of the CIBs for the HDVs are available by using C-V2X infrastructure from the real traffic data. Then, the trajectories of the SCIBs can be estimated by motion planning under the social cost function which will provide the reference information to plan the reference trajectory for the platoon CAVs.

1) Trajectory generation using polynomial curves

The task of the trajectory generation is to provide an obstacle-free path for a vehicle to maintain it in the middle of the lane or, to lead the vehicle from its position to a target position. Regarding the time-critical constraint in vehicle control, the use of search-based or probabilistic approaches for the trajectory planning is not advisable [37]. Among geometric algorithms proposed in the literature, the use of polynomials seems to be a good compromise between simplicity, time computation, trajectory, and curvature continuity, especially in a non-holonomic mobile [38]. To obtain a realistic trajectory model of the lane change in terms of shape and curvature continuity, many works [39], [40] choose a polynomial fifth-degree function to model the longitudinal and lateral dynamics. According to [39], [40], the lateral trajectory concerning the traveling time is expressed as

$$y_{t_i}(t) = q_{t_i}^0 + q_{t_i}^1 t + q_{t_i}^2 t^2 + q_{t_i}^3 t^3 + q_{t_i}^4 t^4 + q_{t_i}^5 t^5, \tag{8}$$

where $y_{t_i}(t)$ is the lateral position of the t_i-th HDV and t is the traveling time such as the intention perception, q^j is the coefficient of the polynomial curve, $j = 1, 2, \ldots, 5$. Define the lateral states of the start point as $Y_{(t_i,st)} = [y_{(t_i,st)}, \dot{y}_{(t_i,st)}, \ddot{y}_{(t_i,st)}, t_{(t_i,st)}]$, where $y_{(t_i,st)}$ is the lateral position at the start point, $\dot{y}_{(t_i,st)}$ and $\ddot{y}_{(t_i,st)}$ are the lateral velocity and acceleration, and $t_{(t_i,st)}$ is the traveling time at the start point. The lateral states $Y_{(t_i,st)}$ can be obtained from the C-V2X infrastructure. Accordingly, define the vehicle lateral states at the end point as $Y_{(t_i,ed)} = [y_{(t_i,ed)}, \dot{y}_{(t_i,ed)}, \ddot{y}_{(t_i,ed)}, t_{(t_i,ed)}]$, where $y_{(t_i,ed)}$ is the lateral position at the end point, $\dot{y}_{(t_i,ed)}$ and $\ddot{y}_{(t_i,ed)}$ are the lateral velocity and acceleration, and $t_{(t_i,ed)}$ is the traveling time at the end point.Then, the coefficient q^j can be computed from vehicle lateral states at the start and end points.

In the normal driving condition, vehicle lateral velocity and lateral acceleration are desired to be zero, i.e., $\dot{y}_{(t_i,ed)} = 0$ and $\ddot{y}_{(t_i,ed)} = 0$. Since the rude and courteous HDVs may reach the end point at different lateral positions and traveling instants, a set of lateral states at the end point can be expressed as follows

$$[y_{(t_i,ed)}, \dot{y}_{(t_i,ed)}, \ddot{y}_{(t_i,ed)}, t_{(t_i,ed)}] = [y_{(t_i,edq)}, 0, 0, t_{(t_i,edq)}], \quad (9)$$

where $y_{(t_i,edq)}$ and $t_{(t_i,edq)}$ are the lateral position and the travelling time at the refernce end point, respectively. We can use the equation (9) to generate possible trajectories by combining different $y_{(t_i,edq)}$ and $t_{(t_i,edq)}$.

The longitudinal trajectory is generated by a similar process. The polynomial curve for the longitudinal trajectory is given by

$$x_{t_i}(t) = p^0_{t_i} + p^1_{t_i}t + p^2_{t_i}t^2 + p^3_{t_i}t^3 + p^4_{t_i}t^4 + p^5_{t_i}t^5, \quad (10)$$

where $x_{t_i}(t)$ is the longitudinal position of the t_i-th HDV, p^j is the coefficient of the polynomial curve and $j = 1, 2, \ldots, 5$. Define the longitudinal states of the start point as $X_{(t_i,st)} = [x_{(t_i,st)}, \dot{x}_{(t_i,st)}, \ddot{x}_{(t_i,st)}, t_{(t_i,st)}]$, where $x_{(t_i,st)}$ is the longitudinal position at the start point, $\dot{x}_{(t_i,st)}$ and $\ddot{x}_{(t_i,st)}$ are the longitudinal velocity and acceleration, and $t_{(t_i,st)}$ is the traveling time at the start point. The longitudinal states $X_{(t_i,st)}$ can be obtained from the C-V2X infrastructure. Accordingly, define the longitudinal states at the end point as $X_{(t_i,ed)} = [x_{(t_i,ed)}, \dot{x}_{(t_i,ed)}, \ddot{x}_{(t_i,ed)}, t_{(t_i,ed)}]$, where $x_{(t_i,ed)}$ is the longitudinal position at the end point, $\dot{x}_{(t_i,ed)}$ and $\ddot{x}_{(t_i,ed)}$ are the longitudinal and acceleration, and $t_{(t_i,ed)}$ is the traveling time at the end point. The vehicle states of the end point are given as the planning targets. Then, the coefficient p^j can be computed from the longitudinal states as the start and the end points, and a set of longitudinal trajectories are generated as the combination of different longitudinal states at the end points.

Based on the generated quintic polynomial curves in both the lateral and longitudinal directions, a set of possible trajectories for rude and courteous HDVs can be established by combining the lateral trajectory $y_{t_i}(t)$ and the longitudinal trajectory $x_{t_i}(t)$.

Remark 4: To ensure the ride comfort and match the driving behaviors, the quintic polynomial curves are employed to generate the jerk-optimal trajectory [39], [40]. Differently, we generate and optimize the trajectory of the HDVs based on the social driving parameters, the dynamic platoon CAVs, the social cost functions, and the extended critical moments which can specifically provide the perception information from the *Observation moment* to identify the vehicles involved in the interaction and the CIIs from the *Prediction moment* to predict the trajectory of CIBs.

2) Collision check and optimal trajectory estimation

The trajectories of the HDVs should avoid possible collisions with the platoon CAVs. Thus, a collision area defined as an ellipse around the *Target vehicle* is shown below

$$(\frac{x_{t_i}(t) - x^*_{t_i}(t)}{a_{r,c}})^2 + (\frac{y_{t_i}(t) - y^*_{t_i}(t)}{b_{r,c}})^2 \leq 1, \quad (11)$$

where $x^*_{t_i}(t)$ and $y^*_{t_i}(t)$ are the real-time predicted longitudinal and lateral positions of the nearby vehicle, respectively, which are obtained from the velocity prediction of the nearby vehicle, i.e., CAV, $a_{r,c}$ is the safe distance to the center of gravity of the nearby CAV in the longitudinal direction and $b_{r,c}$ is that in the lateral direction.

Remark 5: To prevent collisions, the trajectories of the rude and courteous HDVs are not allowed to go beyond the collision area by designing different social driving parameters $a_{r,c}$ and $b_{r,c}$. If a path crosses the collision area, this path will be discarded in the set of possible trajectories for the *Target vehicle*.

Although the trajectories of HDVs are uncertain and hard to determine, the possible paths or trajectories of the HDVs always follow some SDBs. For example, rude HDVs are always aggressive and have near-collision behaviors and courteous HDVs usually want to avoid the near-collision behaviors, which will be defined by different social cost functions. To estimate possible trajectories for HDVs, the trajectory jerk and the deviations to the target state are introduced as the cost function for the lateral candidate trajectories

$$\begin{aligned} J_{(t_i,y)} =& k_1 \int_{t_{(t_i,st)}}^{t_{(t_i,ed)}} \dddot{y}^2_{t_i}(s)ds + k_2(y_{(t_i,edq)} - y_{(t_i,ed)})^2, \\ & s.t. \ k_1 > 0, k_2 > 0, \end{aligned} \quad (12)$$

where $\dddot{y}_{t_i}(t)$ is the lateral jerk of the planned trajectory and k_1, k_2 are two weight parameters. The first item of (12) is the integration of the square of trajectory jerk which is associated with the ride comfort. The second item is the planning error of the target lateral position.

The cost function of the longitudinal trajectory is defined as follows

$$\begin{aligned} J_{(t_i,x)} =& k_3 \int_{t_{(t_i,st)}}^{t_{(t_i,ed)}} \dddot{x}^2_{t_i}(s)ds + k_4(x_{(t_i,edq)} - x_{(t_i,ed)})^2, \\ & s.t. \ k_3 > 0, k_4 > 0, \end{aligned} \quad (13)$$

where k_3, k_4 are two weight parameters and $\dddot{x}_{t_i}(t)$ is the longitudinal jerk of the planned trajectory which is associated with the ride comfort. The second item is planning error to the target longitudinal position.

Then, the total social cost function can be defined as follows

$$\begin{aligned} J_{t_i} =& k_5 J_{(t_i,x)} + k_6 J_{(t_i,y)}, \\ & s.t. \ k_5 > 0, k_6 > 0, \end{aligned} \quad (14)$$

where k_5, k_6 are two social weights for the rude and courteous HDVs. For rude HDVs, $k_5 > k_6$ implies that the HDVs foci on the vehicle traveling at a high speed to compete for the right of way with the platoon CAVs, as the red line shown in Fig. 3. For courteous HDVs, $k_6 > k_5$ represents that the HDVs are more concerned about the safety of traveling at a low speed to avoid near-collision behaviors, as the pink line shown in Fig.3.

Then, the optimal trajectory estimation of the underlying SCIBs of the HDVs can be defined by the following optimization problem

Problem 1 (Optimal trajectory estimation problem):

$$\begin{aligned} & \min_{R_k, C_k = \{k_1,k_2,k_3,k_4,k_5,k_6\}, a_{r,c}, b_{r,c}} J_{t_i} \\ & Subject\ to: \ (1)-(4), (8)-(14), \end{aligned} \quad (15)$$

where R_k and C_k are the weights of the rude and courteous HDVs, and $a_{r,c}$ and $b_{r,c}$ are the social driving parameters, respectively.

Remark 6: Note that the social weights parameters $k_1, \dots, k_6$ can be turned by the realistic traffic data with the help of using regression functions or machine learning methods [25] to identify the SDBs of HDVs. The social driving parameters $a_{r,c}$ and $b_{r,c}$ are usually determined by the driving experience to ensure safety.

IV. Finite state machine of platoon CAVs under social driving environments

By defining the bear bumper of the *Leader CAV* as a reference, all the roles of the SVs will be determined as the *Front-vehicles*, *Rear-vehicles*, or *Target-vehicles* according to the relative positions of HDVs, where the roles of the SVs are dynamically changed due to uncontrolled trajectories of the HDVs. Then, this paper aims to design an efficient platoon control strategy to prevent the possible SCIBs of the *Target vehicles* according to the estimated trajectories of HDVs. Considering different driving scenarios, four classes of platoon states are defined to construct the ADMDSS as shown in Fig. 4.

*Definition 9 (STATE 1-*Cruising*):* For any rude or courteous HDV, if the longitudinal distance with respect to the platoon CAVs is longer than a given safe cruising distance, the traveling behaviors of the platoon CAVs will not be affected by the HDV, and the platoon CAVs will be in the *STATE 1-Cruising*, i.e., $F(t) = 0$. The cruising distance is given by:

$$\begin{aligned}
D =& ||x(t) - s_{(0,x)}(t)|| > D_c, \\
D_c =& D_{(c,0)} + \hat{\beta}(v_{(0,x)}(t) + \frac{1}{N}\sum_{j=1}^{N}\alpha(v_{(j,x)}(t) - v_{(i,x)}(t))), \\
D_{(c,0)} =& D_{cs} + (2 \times l_c) \times N + D_s, \\
D_s =& D_{i0} + h_{i0}v_{(i,x)}(t), i = N, \\
D_{cs} >& \hat{\kappa}(D_s + (2 \times l_c) \times N),
\end{aligned} \tag{16}$$

where D_c is designed by the combination of the cruising distance and velocity, D_{cs} is the basic safe distance called as the longitudinal cruising external-space distance, $v_{(0,x)}(t)$ and $v_{(i,x)}(t)$ are the longitudinal velocities of the *Leader CAV* and *Follower CAVs*, $\hat{\beta}$ is the velocity factor of cruising distance, α is the coupling weight among the CAVs, D_s is designed by the velocity-dependent spacing policy, D_{i0} is the standstill safe distance between the CAVs i and 0, h_{i0} is the constant time headway, l_c is the half longitudinal length of the vehicle, $\hat{\kappa}$ is a scalar, and N is the number of the *Follower CAVs*.

*Definition 10 (STATE 2-*Following control*):* The displacements of the specific HDV compared with the *Leader CAV* are as follows:

$$\begin{aligned}
y_{ep} =& ||(y(t_e) - y(t_p)) - (s_{(0,y)}(t_e) - s_{(0,y)}(t_p))||, \\
x_{ep} =& ||(x(t_e) - x(t_p)) - (s_{(0,x)}(t_e) - s_{(0,x)}(t_p))||,
\end{aligned} \tag{17}$$

Then, the platoon will adjust the cooperative control strategy to maintain a safe cruising distance from the HDVs, if the relative position between the specific HDV and the platoon CAVs meets the following constraint

$$D_w < x_{ep} = D \leq D_c, y_{ep} = H > H_l, \tag{18}$$

where D_w and H_l are the traveling distances, which will be described in detail in the following. In this case, the platoon will be in the *STATE 2-Following control*, i.e., $F(t) = 1$.

*Definition 11 (STATE 3-*Real-time tracking control*):* If the HDV is courteous, the platoon will accelerate to switch into the *STATE 3-Real-time tracking control*, i.e., $F(t) = 2$, following a high-speed reference to prevent the CIBs of the HDV, when the longitudinal distance between the platoon CAVs and the HDV is within the range

$$\begin{aligned}
x_{ep} \leq& D_w, \\
D_w =& D_{(w,0)} + \frac{\hat{\gamma}}{2}(v_{(0,x)}(t_p) \\
&+ \frac{1}{N}\sum_{j=1}^{N}\alpha(v_{(j,x)}(t_p) - v_{(i,x)}(t_p) \\
&+ v_{(0,x)}(t_e) + \frac{1}{N}\sum_{j=1}^{N}\alpha(v_{(j,x)}(t_e) - v_{(i,x)}(t_e)), \\
D_{(w,0)} =& \begin{cases} D_{ws} + (2 \times l_c) \times N + D_s, \text{Case1;} \\ D_{ws} + (2 \times l_c) \times N^* + D_s^*, \text{Case2,} \end{cases} \\
D_s^* =& D_{i0} + h_{i0}v_{(i,x)}(t), i = N^*, \\
D_{cw} \leq& \hat{\kappa}(D_s + 2 \times l_c),
\end{aligned} \tag{19}$$

and the lateral distance satisfies the following condition

$$\begin{aligned}
H_h \leq& y_{ep} \leq H_l, \\
H_h =& H_{(h,0)} + \frac{\hat{\zeta}}{2}(v_{(0,y)}(t_p) \\
&+ \frac{1}{N}\sum_{j=1}^{N}\alpha(v_{(j,y)}(t_p) - v_{(i,y)}(t_p) \\
&+ v_{(0,y)}(t_e) + \frac{1}{N}\sum_{j=1}^{N}\alpha(v_{(j,y)}(t_e) - v_{(i,y)}(t_e)),
\end{aligned} \tag{20}$$

where D_{ws} is the basic safe distance called the longitudinal tracking external-space distance, $\hat{\gamma}$ is the velocity factor of traveling distance, H_h is the lateral traveling distance, H_{h0} is the basic safe distance called the lateral external-space distance, $\hat{\zeta}$ is the velocity factor of traveling distance, Case 1 and Case 2 represent the HDVs to be the *Target vehicles*, and N and N^* are the full and part numbers of platoon CAVs in the front of the specific *Target vehicle*, respectively.

*Definition 12 (STATE 4-*Avoidance in advance*):* If the HDV is rude or the CIIs show that the HDV may drive into the following range

$$x_{ep} < D_w, y_{ep} < H_h, \tag{21}$$

the platoon CAVs will decelerate to switch into the *STATE4-Avoidance in advance*, i.e., $F(t) = 3$, following a low-speed reference to prevent the SCIBs of the HDVs or reduce the

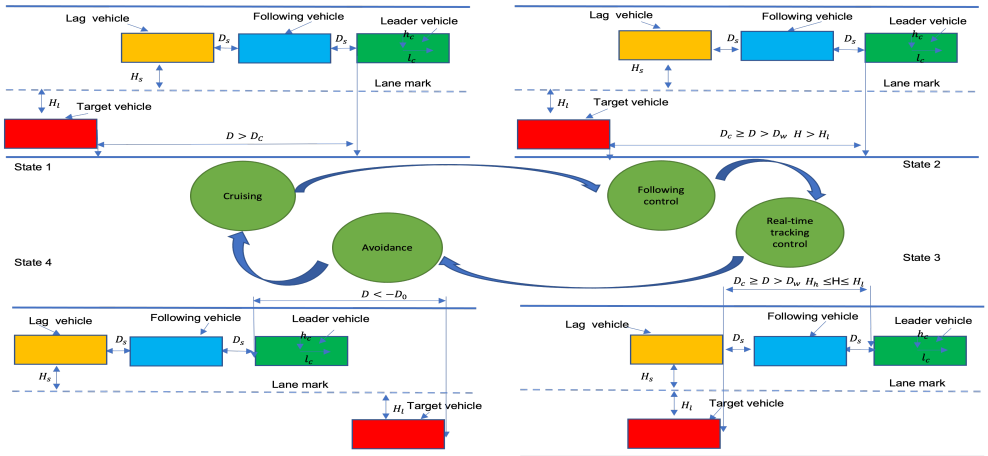

Fig. 4. Finite state machine of platoon states in the ADMDSS.

influence of the LCBs of the HDVs to ensure safety so that the inter-space distance satisfies

$$D_{i0} + h_{i0}v_{(i,x)}(t) \approx l_0, \tag{22}$$

where l_0 is a minimum distance to prevent the CIBs of the HDVs.

Notably, determining the traveling state of the platoon CAVs is mainly based on the traveling distance between the platoon CAVs and the HDVs and the optimal trajectory estimation of possible SCIBs for the HDVs. The detailed strategy transition of finite state machine among four states for the ADMDSS is shown in Algorithm 1.

Remark 7: By combining the relative traveling distances and the weighted velocity errors, the finite state machine decision algorithm provides an automatic decision-making framework to determine the roles of SVs and the relationship between the HDVs and the platoon CAVs so that the cooperative driving and optimization for the platoon CAVs can be respectively implemented for the specific driving scenarios under different SDBs of the HDVs.

V. Platoon control and optimization against SCIBs

A. Reference trajectory planning

Based on the above finite state machine of platoon CAVs with respect to the possible SCIBs of the HDVs, the reference trajectory of the *Leader CAV* will be planned by developing the following reference velocity design criterions for the ADMDSS to keep a safe external-space distance from the HDVs and adjust the inter-space distance to prevent the underlying SCIBs of the HDVs.

*Criterion 1 (**C-I**):* In the *STATE 1-Cruising*, the velocity of the platoon CAVs will not be affected by the HDVs due to the large external-space distance. Then, the reference trajectory planning of the *Leader CAV* will be determined by a cruising velocity $v_{tra}(t)$

$$v_{tra}(t) = v_c, \tag{23}$$

where v_c is the designed cruising velocity by using the C-V2X infrastructure according to the schedule demands.

*Criterion 2 (**C-II**):* In the *STATE 2-Following control*, the HDVs will approach the platoon CAVs. Then, the reference trajectory planning of the *Leader CAV* is to expect to maintain the following safe external-space distance with respect to the specific HDV

$$D_f \geq D_{f0} + \mu \dot{x}^t, \tag{24}$$

where $\dot{x}^t$ is the velocity of the specific HDV at time t, D_f is the reference following distance, D_{f0} is a basic following distance, and μ is the velocity factor of the following distance. Then, the longitudinal reference velocity is planned as follows:

$$v^{t^+}_{(tra,x)} = \dot{x}^t + \hat{\delta}(s^t_{(0,x)} - x^t - (2 \times l_c) \times N - D_s - D_f), \tag{25}$$

where $v^{t^+}_{(tra,x)}$ is the longitudinal reference velocity at time t, x^t and $s^t_{(0,x)}$ are the longitudinal positions of the specific HDV and the *Leader CAV*, respectively, $\hat{\delta} > 0$ is a velocity adjustment factor. In this case, we consider the lateral velocity as zero. The reference velocity can be described as follows:

$$v_{tra}(t) = [v^{t^+}_{(tra,x)}, 0]. \tag{26}$$

*Criterion 3 (**C-III**):* In the *STATE 3-Real-time tracking control*, for the courteous HDVs, the platoon will drive first to prevent the SCIBs of the HDVs. To avoid the collision, the longitudinal displacement of the *Leader CAV* should satisfy the following condition

$$\begin{aligned} & s_{(0,x)}(t_e) - x_{t_p} \geq D_g, \\ & D_g = \begin{cases} s_{(0,x)}(t_e) - s_{(0,x)}(t_p) + (x_{t_e} - x_{t_p}) + D_f \\ \quad + (2 \times l_c) \times N + D_s, Case3; \\ s_{(0,x)}(t_e) - s_{(0,x)}(t_p) + (x_{t_e} - x_{t_p}) + D_f \\ \quad + (2 \times l_c) \times N^* + D_s^* \\ \quad + x_{t_p} - (s^N_{(0,x)}(t_p)), Case4, \end{cases} \\ & s^N_{(0,x)}(t_p) = s_{(0,x)}(t_p) - (2 \times l_c) \times N - D_s - 2 \times l_c, \end{aligned} \tag{27}$$

Algorithm 1 Finite state machine decision algorithm

Input: t_0, t_p, $\hat{\beta}$, $\hat{\gamma}$, $\hat{\zeta}$, $\hat{\kappa}$, h_{i0}, l_c, l_0,α, N, N^*, the driving state $F(t)$, the longitudinal distance D and the lateral distance H between the HDVs and the platoon CAVs; **Output:** The driving state $F(t)$.

if $F(t) = 0$ **then**
  if $D \leq D_w$ **then**
    if HDV is cutaneous and $H_h \leq H \leq H_l$ **then** $F(t) = 2$;
    else HDV has rude SCIB and $H < H_h$ $F(t) = 3$;
    end if
  else if $D_w < D \leq D_c$ and $H > H_l$ **then** $F(t) = 1$;
  else $F(t) = 0$;
  end if
else if $F(t) = 1$ **then**
  if $D \leq D_w$ **then**
    if HDV is cutaneous and $H_h \leq H \leq H_l$ **then** $F(t) = 2$;
    else HDV has rude SCIB or $H < H_h$ $F(t) = 3$;
    end if
  else if $D > D_c$ **then** $F(t) = 0$;
  else $F(t) = 1$;
  end if
else if $F(t) = 2$ **then**
  if $D \leq D_w$ **then**
    if HDV is cutaneous and $H_h \leq H \leq H_l$ **then** $F(t) = 2$;
    else HDV has rude SCIB or $H < H_h$ $F(t) = 3$;
    end if
  else $F(t) = 1$;
  end if
else if $F(t) = 3$ **then**
  if $D \leq D_w$ **then**
    if HDV is cutaneous and $H_h \leq H \leq H_l$ **then** $F(t) = 2$;
    else HDV has rude SCIB or $H < H_h$ $F(t) = 3$;
    end if
  else $F(t) = 2$.
  end if
end if

where Case 3 and Case 4 represent the different positions of the *Target vehicles*. For details, in Case 3, the longitudinal position of the *Target vehicle* is the same as the *Lag CAV* in the platoon, and Case 4 represents the rest of the cases. It is assumed that the platoon CAVs are planned to move with uniform acceleration. Then, the longitudinal reference velocity is planned as follows:

$$v^{\top}_{(tra,x)} = v^{\top}_{(0,x)} + \frac{D_g - D_t - D_b}{t_e - (t - t_p)}. \tag{28}$$

where D_b is a safe buffer for the longitudinal reference. During the process of the lateral transmission, the moving between the platoon CAVs and the specific HDV is given by

$$s_{(0,y)}(t_e) - y_{t_p} \geq s_{(0,y)}(t_e) - s_{(0,y)}(t_p) + y_{t_e} - y_{t_p} + H_h, \tag{29}$$

which implies that

$$s_{(0,y)}(t_p) - y_{t_e} \geq H_h, \tag{30}$$

where the platoon CAVs will not actively approach the HDVs. Then, the lateral reference velocity is planned as follows:

$$v^{\top}_{(tra,y)} = v^{\top}_{(0,y)} + \frac{H_h - H_t - H_b}{t_e - (t - t_p)}. \tag{31}$$

where H_b is a safe buffer for the lateral reference. Therefore, the reference velocity can be described as follows:

$$v_{tra}(t) = [v^{\top}_{(tra,x)}, v^{\top}_{(tra,y)}]. \tag{32}$$

*Criterion 4 (**C-IV**):* In the *STATE 4-Avoidance in advance*, the platoon will decelerate to reduce the inter-space distance to prevent the SCIBs of the HDVs and maintain a safe distance from the HDVs. To avoid a collision, we may obtain the crossover target point of the longitudinal trajectory of the *Leader CAV* and the predicted trajectory of the specific HDV, defined as O, by using the C-V2X infrastructure. Then, it is expected to maintain a safe distance D_o as follows:

$$D_o = D_{o0} + \mu_o \dot{x}, \tag{33}$$

where D_{f0} is the basic safe distance, and μ_o is the velocity factor of the following control distance. Then, the longitudinal displacement of the *Leader CAV* should satisfy the following condition

$$\begin{aligned} & x_{t_e} - x_{t_p} \geq D_k, \\ & D_k = \begin{cases} s_{(0,x)}(t_p) - x_{t_p} + s_{(0,x)}(t_e) - s_{(0,x)}(t_p) + D_o \\ \quad + (2 \times l_c) \times N + D_s + 2 \times l_c, Case3; \\ s_{(0,x)}(t_p) - x_{t_p} + s_{(0,x)}(t_e) - s_{(0,x)}(t_p) + D_o, \\ \quad + (2 \times l_c) \times N^* + D_s^* + 2 \times l_c \\ \quad - x_{t_p} - s^N_{(0,x)}(t_p), Case4. \end{cases} \end{aligned} \tag{34}$$

Then, the longitudinal reference velocity is planned as follows:

$$v^{t^-}_{(tra,x)} = v^{\top}_{(0,x)} + \frac{D_k - D_o - D_t - D_b}{t_e - (t - t_p)}. \tag{35}$$

In this case, we consider the lateral velocity as zero. The reference velocity can be described as follows:

$$v_{tra}(t) = [v^{t^-}_{(tra,x)}, 0]. \tag{36}$$

B. Controller design for dynamic platoon management

The controller design contains the acceleration planning for the *Leader CAV* under **C-I-C-IV** and the cooperative controller developing for the *Follower CAVs*. It is noted that the velocity adjusting of the *Leader CAV* shall consider the platoon economy and safety. If the platoon is traveling with a constant velocity v_c under **C-I**, the acceleration of the *Leader CAV* will be zero at the *Prediction moment* t_p. Our aim is to adjust the platoon velocity in the time interval $[t_p, t_e]$ to ensure that the platoon reaches the planning demands to prevent the possible SCIBs of the HDVs. In general, we can use the maximum acceleration to adjust the traveling velocity to reach the reference velocity under **C-II-C-IV**. However, it may cause a risk of driving safety. Therefore, we will try to design an optimal regulation time $\hat{T}$, where $\hat{T} \leq t_{ep}$ with $t_{ep} = t_e - t_p$ being a time interval between the *Prediction moment* and the *End moment*, which is associated with the reference velocity adjustment and the stability of the platoon with the reference trajectory under **C-II-C-IV** in a finite time. Notably, $\hat{T}$ is free for the *Cruising state* because the *Leader CAV* will maintain the constant cruising velocity under **C-I**. For other cases, since the *Leader CAV* adjusts the status first under **C-II-C-IV** and then all the *Follow vehicles* track the preceding CAVs, the option of the finite time $\hat{T}$ will be the key factor to ensure the safety of the platoon and prevent the underlying SCIBs of the HDVs. To simplify, we ignore the indexes for the longitudinal and lateral dynamics because the lateral controller design can be regarded as a specific case.

To determine the optimal and economic adjusting of the *Leader CAV* under **C-II-C-IV**, the following optimization problem is first investigated, which ignores the influence of the small differences in the vehicle cruising speed on energy consumption in a congested traffic environment.

Problem 2 (Fuel economic optimisation problem):

$$\begin{aligned} \min J &= \int_0^{t_{ep}} a^2(\tau) d\tau \\ \text{Subject to :} & v_0(0) + \int_0^{t_{ep}} a_0(\tau) d\tau = v_0(t_{ep}). \end{aligned} \tag{37}$$

where $v_0(0)$, $v_0(t_{ep})$ and t_{ep} can be estimated by solving the optimal trajectory estimation problem (15). Then, the function of a_0 will be optimally determined.

This is a standard variational problem with an equality constraint. We can easily check that the optimal solution is

$$a_0^*(t) = \frac{v_0(t_{ep}) - v_0(0)}{t_{ep}}, \tag{38}$$

that is, a constant acceleration will lead to the minimum fuel consumption in $[t^*, t^* + t_{ep}]$. The resulting fuel consumption is

$$J_a^* = \int_0^{t_{ep}} (a_0^*(\tau))^2 d\tau = \frac{(v_0(t_{ep}) - v_0(0))^2}{t_{ep}}, \tag{39}$$

which means the larger the value t_{ep}, the smaller the fuel consumption.

Based on the above analysis, the *Leader CAV* needs to use a constant acceleration $\frac{(v_{tra}(t)-v_0(0))}{t_*}$ to reach the reference velocity $v_{tra}(t)$ under **C-II-C-IV** as an economical acceleration adjusting under the sufficient regulation time t_* that satisfies

$$\begin{aligned} \zeta\delta &\le a_{max}, \\ t_* &= \frac{(v_{tra}(t) - v_0(0))}{\delta}, \end{aligned} \tag{40}$$

where $\zeta > 0$ is a regulation parameter to value the compromise between driving safety and energy consumption, and it generally takes the value $[1, 10]$ for the comfort level of driving into account.

Therefore, the economic acceleration adjusting scheme is selected by a constant value during $[0, t_{ep}]$. According to the dynamic (7), the acceleration profile of the *Leader CAV* under **C-II-C-IV** can be designed by

$$u_0(t) = \frac{(v_{tra}(t) - v_0(0))}{t_*}. \tag{41}$$

Based on the above procedures, the nonlinear decision function $f(F(t), u_0(t))$ will be constructed by the finite state function $F(t) = \{0, 1, 2, 3\}$, the reference velocity $v_{tra}(t)$, and the economical acceleration adjusting (41). Notably, when the *Leader CAV* achieves the planning demands, all the *Follower CAVs* will need to form the platoon and ensure the safe distance in a finite time $\hat{T}$. Therefore, the control horizon will need to be satisfied in the following constraints

$$\begin{cases} \hat{T} = t_*, & if\ \ddot{x} = 0, \\ \hat{T} < t_e - t_p + t_*, & if\ \ddot{x} \neq 0, \end{cases} \tag{42}$$

where the first case is for the *STATE 2-Following control* and the second case covers the *STATE 3-Real-time tracking control* and the *STATE 4-Avoidance in advance*, respectively.

Notably, the control execution varies depending on the role of the current vehicles. For the *STATE 1-Cruising*, the control action aims to form the platoon due to the large external-space distance with respect to the HDVs. For the *STATE 2-Following control*, the control action will need to maintain the following safe external-space distance with respect to the specific HDV. The main difference of the control actions between *STATE 3-Real-time tracking control*, and *STATE 4-Avoidance in advance* is different reference trajectory planning for the *Leader CAV* due to different roles of the *Target vehicles*. Then, the following two criterions are proposed to design the cooperative controller for the *Follower CAVs* in different driving scenarios, respectively

*Criterion 5 (**C-V**):* For the *Leader CAV* having the constant cruising velocity under **C-I**, the following controllers are designed for the *STATE 1-Cruising*

$$\begin{aligned} u_i(t) =& cK_1 \sum_{j=0}^{N} \alpha_{ij} (s_j(t) - s_i(t) + (j-i) \times (2 \times l_c) \\ &+ D_{ij} + h_{ij} v_j(t) + h_{i0}(v_j(t) - v_i(t))) \\ &+ cK_2 \sum_{j=0}^{N} \alpha_{ij} (v_j(t) - v_i(t)) + cK_3 \sum_{j=0}^{N} \alpha_{ij} (a_j(t) - a_i(t)), \\ y_i(t) =& \hat{\alpha} \sum_{j=0}^{N} \alpha_{ij} \left[V_i(y_{ij}(t)) - v_i(t) \right], \\ g_i(t) =& \bar{\alpha} \sum_{j=0}^{N} \alpha_{ij} (v_j(t) - v_i(t)), i \in \mathbb{F}, \end{aligned} \tag{43}$$

where $D_{ij} = D_{j0} - D_{i0}$, $h_{ij} = h_{j0} - h_{i0}$, K_1, K_2, K_3 are the feedback gains, $c > 0$ is the coupling gain, and $A = [\alpha_{ij}]_{(N+1)\times(N+1)}$ is the adjacency matrix of graph G. Specially, $\hat{\alpha}$ and $\bar{\alpha}$ are the sensitivity constants, and $V_i(y_{ij}(t))$ is the nonlinear reaction function, also named as "Optimal Velocity Function (OVF)" [13], [41], [42], to capture the interactions between CAVs i and j, as shown below

$$V_i\left(y_{ij}\left(t\right)\right) = D_1 + D_2 \tanh\left(D_3\left(y_{ij}\left(t\right)\right) - D_4\right), \tag{44}$$

where D_1, D_2, D_3, D_4 are four positive constants. The average bumper-to-bumper distance $y_{ij}(t)$ between CAVs i and j can be given by:

$$y_{ij}(t) = \left(s_j(t) - s_i(t)\right) / \left(j - i\right), i, j \in \mathbb{F}. \tag{45}$$

*Criterion 6 (**C-VI**):* For the *Leader CAV* having unknown planning demands under **C-II-C-IV** that are associated with uncertain HDVs in the other three finite states, i.e., *STATE 2-Following control*, *STATE 3-Real-time tracking control*, and *STATE 4-Avoidance in advance*, the following controllers are further designed

$$\begin{aligned}
\hat{u}_i(t) =& \xi_i(t) + u_i(t) \\
&+ \hat{c}sgn(K_1 \sum_{j=0}^{N} \alpha_{ij}(s_j(t) - s_i(t) + (j-i) \times (2 \times l_c) \\
&+ D_{ij} + h_{ij}v_j(t) + h_{i0}(v_j(t) - v_i(t))) \\
&+ K_2 \sum_{j=0}^{N} \alpha_{ij}(v_j(t) - v_i(t)) + K_3 \sum_{j=0}^{N} \alpha_{ij}(a_j(t) - a_i(t))), \\
\dot{\xi}_i(t) =& \xi_i\left(t\right) + cQ \sum_{j=0}^{N} a_{ij}\left(\xi_j\left(t\right) - \xi_i\left(t\right)\right) \\
&+ c_0 \mathrm{sgn}\left(Q \sum_{j=0}^{N} a_{ij}\left(\xi_j\left(t\right) - \xi_i\left(t\right)\right)\right), i \in \mathbb{F},
\end{aligned} \tag{46}$$

where $\xi_i(t) \in \mathbb{R}^n$ is the distributed estimation of the i-th *Follower CAV* for the *Leader CAV*'s acceleration and $\xi_0(t) = a_0(t)$, c_0 is the coupling gain, $\hat{c} > 0$ is a scalar, and Q is the observer gain which will be designed later.

C. Stability analysis of dynamic platoon management

Since the *Cruising state* is a special case of the finite state machine in the ADMDSS, the stability analysis of the platoon under the controller (46) with **C-VI** can cover all the switching states. Then, define the platoon error as follows:

$$\begin{cases}
\tilde{s}_i(t) = s_i(t) - s_0(t) + i \times (2 \times l_c) + D_{i0} + h_{i0}v_i(t), \\
\tilde{v}_i(t) = v_i(t) - v_0(t), \\
\tilde{a}_i(t) = a_i(t) - a_0(t). \\
\tilde{\xi}_i(t) = \xi_i(t) - \xi_0(t), i \in \mathbb{F}.
\end{cases} \tag{47}$$

By defining $y_{ij}^*(t) = \frac{(j-i)\times(2\times l_c)+D_{ij}+h_{ij}v_j(t)+h_{i0}(v_j(t)-v_i(t))}{j-i}$ and $V_i(y_{ij}^*(t)) = v_0(t)$, it follows from (46) that

$$\begin{aligned}
y_i(t) =& \hat{\alpha} \sum_{j=0}^{N} \alpha_{ij}\left[V_i(y_{ij}(t)) - V_i(y_{ij}^*(t)) + V_i(y_{ij}^*(t)) - v_i(t)\right] \\
=& \hat{\alpha} \sum_{j=0}^{N} \alpha_{ij}\left[V_i(y_{ij}(t)) - V_i(y_{ij}^*(t)) - \tilde{v}_i(t)\right], i \in \mathbb{F}.
\end{aligned} \tag{48}$$

Specifically, it follows (48) that

$$V_i\left(y_{ij}(t)\right) = V_i\left(y_{ij}^*(t)\right) + V_i^{'}\left(y_{ij}^*(t)\right)\left(y_{ij}(t) - y_{ij}^*(t)\right), i \in \mathbb{F}. \tag{49}$$

Based on (49), we have

$$\begin{aligned}
& V_{\mathrm{i}}(y_{ij}(t)) - V_i(y_{ij}^*(t)) \\
=& V_i^{'}(y_{ij}^*(t))((s_j(t) - s_i(t))/(j-i) - y_{ij}^*(t)) \\
=& \frac{V_i^{'}(y_{ij}^*(t))(s_j(t) - s_i(t) + y_{ij}^*(t))}{(i-j)} \\
=& \frac{V_i^{'}(y_{ij}^*(t))(\tilde{s}_j(t) - \tilde{s}_i(t))}{(i-j)} \\
=& \phi_{ij}(t)(\tilde{s}_j(t) - \tilde{s}_i(t)), i \in \mathbb{F},
\end{aligned} \tag{50}$$

where $\phi_{ij}(t) = V_i^{'}(y_{ij}^*(t))/(i-j)$.

It follows from (6), (7), (46) - (47) that

$$\begin{cases}
\dot{\tilde{s}}_i(t) = \tilde{v}_i(t) + h_{i0}a_i(t), \\
\dot{\tilde{v}}_i(t) = \tilde{a}_i(t), \\
\dot{\tilde{a}}_i(t) = -\frac{1}{\tau}\tilde{a}_i(t) + \frac{1}{\tau}\tilde{\xi}_i(t) + \frac{1}{\tau}a_0(t) - \frac{1}{\tau}\delta \\
\quad - \frac{1}{\tau}\Big(cK_1 \sum_{j=0}^{N} \alpha_{ij}(\tilde{s}_i(t) - \tilde{s}_j(t)) \\
\quad + cK_2 \sum_{j=0}^{N} \alpha_{ij}(\tilde{v}_i(t) - \tilde{v}_j(t)) + cK_3 \sum_{j=0}^{N} \alpha_{ij}(\tilde{a}_i(t) - \tilde{a}_j(t))\Big) \\
\quad - \frac{\hat{c}}{\tau}sgn\Big(K_1 \sum_{j=0}^{N} \alpha_{ij}(\tilde{s}_i(t) - \tilde{s}_j(t)) \\
\quad + K_2 \sum_{j=0}^{N} \alpha_{ij}(\tilde{v}_i(t) - \tilde{v}_j(t)) + K_3 \sum_{j=0}^{N} \alpha_{ij}(\tilde{a}_i(t) - \tilde{a}_j(t))\Big) \\
\quad - \frac{\hat{\alpha}}{\tau} \sum_{j=0}^{N} \alpha_{ij}\left[\phi_{ij}(t)(\tilde{s}_i(t) - \tilde{s}_j(t)) + \tilde{v}_i(t)\right] \\
\quad - \frac{\bar{\alpha}}{\tau} \sum_{j=0}^{N} \alpha_{ij}((\tilde{v}_i(t) - \tilde{v}_j(t))), \\
\dot{\tilde{\xi}}_i(t) = \tilde{\xi}_i(t) + cQ \sum_{j=0}^{N} a_{ij}\left(\tilde{\xi}_j\left(t\right) - \tilde{\xi}_i\left(t\right)\right) \\
\quad + c_0 \mathrm{sgn}\left(Q \sum_{j=0}^{N} a_{ij}\left(\tilde{\xi}_j\left(t\right) - \tilde{\xi}_i\left(t\right)\right)\right) \\
\quad + \frac{1}{\tau}a_0(t) + a_0(t) - \frac{1}{\tau}\delta, i \in \mathbb{F}.
\end{cases} \tag{51}$$

To analyze the stability, we would like to introduce the following variables $\chi_i(t) = [\tilde{s}_i(t), \tilde{v}_i(t), \tilde{a}_i(t)]$, $i \in \mathbb{F}$. Then, we have the following platoon dynamics

$$\begin{aligned}
\dot{\chi}_i(t) =& A\chi_i(t) + Cf(\chi_i(t), t) + T_2\tilde{\xi}_i(t) + T_2(a_0(t) - \delta) \\
&+ BU_i(t) + \hat{c}Bsgn(\hat{U}_i(t)) + A_{i0}a_i(t), i \in \mathbb{F},
\end{aligned} \tag{52}$$

where $A = \begin{bmatrix} 0 & 1 & 0 \\ 0 & 0 & 1 \\ 0 & 0 & -\frac{1}{\tau} \end{bmatrix}$, $B = \begin{bmatrix} 0 \\ 0 \\ \frac{1}{\tau} \end{bmatrix}$, $C = I_3$, $T_2 = [0, 0, \frac{1}{\tau}]^\top$, $A_{i0} = [h_{i0}, 0, 0]^\top$, and

$$
\begin{aligned}
U_i(t) = &-(cK_1 \sum_{j=0}^{N} \alpha_{ij}(\tilde{s}_i(t) - \tilde{s}_j(t)) + cK_2 \sum_{j=0}^{N} \alpha_{ij}(\tilde{v}_i(t) - \tilde{v}_j(t)) \\
&+ cK_3 \sum_{j=0}^{N} \alpha_{ij}(\tilde{a}_i(t) - \tilde{a}_j(t))), \\
\hat{U}_i(t) = &-(K_1 \sum_{j=0}^{N} \alpha_{ij}(\tilde{s}_i(t) - \tilde{s}_j(t)) + K_2 \sum_{j=0}^{N} \alpha_{ij}(\tilde{v}_i(t) - \tilde{v}_j(t)) \\
&+ K_3 \sum_{j=0}^{N} \alpha_{ij}(\tilde{a}_i(t) - \tilde{a}_j(t))), \\
f(t) = &[0, 0, \mathcal{Y}_3(t)]^\top, \\
\mathcal{Y}_3(t) = &-\frac{\hat{\alpha}}{\tau} \sum_{j=0}^{N} \alpha_{ij} \left[\phi_{ij}(t)(\tilde{s}_i(t) - \tilde{s}_j(t)) + \tilde{v}_i(t)\right] \\
&- \frac{\bar{\alpha}}{\tau} \sum_{j=0}^{N} \alpha_{ij}((\tilde{v}_i(t) - \tilde{v}_j(t))).
\end{aligned}
$$

To obtain the results, the following assumption and lemma are introduced.

Assumption 1: The communication topology contains a directed spanning tree with the *Leader CAV* as a root node.

With Assumption 1, the Laplacian matrix L associated with the topology G can be written as the following form

$$
L = \begin{pmatrix} 0 & 0_N^\top \\ L_0 & L_1 \end{pmatrix}, \tag{53}
$$

where $L_0 \in \mathbb{R}^N$, $L_1 \in \mathbb{R}^{N \times N}$.

Lemma 1: [43] With Assumption 1, there exists a positive vector $\theta = (\theta_1, \cdots, \theta_N)^\top \in \mathbb{R}^N$, such that $L_1 \theta = 1_N$ and

$$
\Theta L_1 + (L_1)^\top \Theta > 0, \tag{54}
$$

where $\Theta = diag\{1/\theta_1, \cdots, 1/\theta_N\}$, for all $t \geq 0$.

Furthermore, define $\tilde{\xi} = [\tilde{\xi}_1^\top, \ldots, \tilde{\xi}_N^\top]$. Based on (51), we have

$$
\begin{aligned}
\dot{\tilde{\xi}}(t) = &(I_N \otimes I_N)\, \tilde{\xi}(t) - c\,(L_1 \otimes Q)\, \tilde{\xi}(t) \\
&- c_0\,(I_N \otimes I_N) \operatorname{sgn}\left((L_1 \otimes Q)\, \tilde{\xi}(t)\right) \\
&+ (I_N \otimes I_N)\, \breve{a}(t),
\end{aligned} \tag{55}
$$

where $\breve{a}(t) = \frac{1}{\tau} a_0(t) + a_0(t) - \frac{1}{\tau}\delta \leq (1 + \frac{1}{\tau}) a_{max}$.

Then, by defining $\chi(t) = [\chi_1^\top, \ldots, \chi_N^\top(t)]^\top$, the error dynamics of platoon can be rewritten by the following compact form

$$
\begin{aligned}
\dot{\chi}(t) = &(I_N \otimes A)\, \chi(t) + (I_N \otimes T_2)\, \tilde{\xi}(t) + (I_N \otimes T_2)\, \acute{a}(t) \\
&- (L_1 \otimes M_1)\, \chi(t) - (L_1 \otimes M_2)\, \chi(t) \\
&- (D \otimes M_3)\, \chi(t) - c\,(L_1 \otimes BK)\, \chi(t) \\
&- \hat{c}\,(I_N \otimes I_N) \operatorname{sgn}((L_1 \otimes BK)\, \chi(t))
\end{aligned} \tag{56}
$$

where $\acute{a}(t) = a_0(t) - \delta + \frac{\lambda_{\max}(h_{i0})}{\frac{1}{\tau}} a_i(t) \leq b a_{max}$, $b = 1 + \frac{\lambda_{\max}(h_{i0})}{\frac{1}{\tau}}$, $M_1 = \begin{bmatrix} 0 & 0 & 0 \\ 0 & 0 & 0 \\ \frac{\hat{\alpha}\phi_{ij}(t)}{\tau} & 0 & 0 \end{bmatrix}$, $M_2 = \begin{bmatrix} 0 & 0 & 0 \\ 0 & 0 & 0 \\ 0 & \frac{\bar{\alpha}}{\tau} & 0 \end{bmatrix}$, $M_3 = \begin{bmatrix} 0 & 0 & 0 \\ 0 & 0 & 0 \\ 0 & \frac{\hat{\alpha}}{\tau} & 0 \end{bmatrix}$, $K = [\ K_1 \quad K_2 \quad K_3\ ]$, $D = diag\{d_i\} \in \mathbb{R}^{N \times N}$ is the in-degree matrix.

Then, we present the first result for the dynamic platoon management for an infinite time horizon and the finite-time convergence solution is obtained by proposing a robust cooperative trajectory tracking optimization which will be discussed later.

Theorem 1: With Assumption 1, the dynamic platoon management problem is solved for an infinite time horizon by the protocols (43) and (46) under **C-V-C-VI** and the finite state function $F(t)$ with the feedback gains $K = \kappa B^\top P^{-1}$ and the observer gain $Q = T^{-1} P_0$, if the following equations have feasible solutions

$$
P_0 + P_0^\top - \omega \theta_0 P_0 Q = -I_n, \tag{57}
$$

$$
\begin{aligned}
&AP + PA^\top - \lambda_0 \theta_0 M_1 P - \lambda_0 \theta_0 M_2 P \\
&- 2 d_0 M_3 P - \omega \theta_0 \kappa B B^\top + \beta P < 0,
\end{aligned} \tag{58}
$$

where $\kappa > 0$ and $\beta > 0$ are two scalars, $\theta_0 = \min \theta_i$ with θ_i being given in Lemma 1, $d_0 = \min d_i$, $\omega > 0$ is a coupling design parameter, P_0 is the positive definite matrix, $T = T^\top \in R^{n \times n}$ is to be selected positive definite matrix. Moreover, choosing the coupling strength $c_0 = (1 + \frac{1}{\tau}) a_{max}$, $\hat{c} c_1 = b a_{max} c_2$ with $b = 1 + \frac{\lambda_{\max}(h_{i0})}{\frac{1}{\tau}}$, $c_1 = \lambda_{min}((BB^\top)^\top / \kappa)$, $c_2 = \lambda_{min}((BB^\top)^\top / \kappa T_2)$, $c > \omega / \lambda_0$, where $\lambda_0 = \lambda_{\min}(\Theta L_1 + (L_1)^\top \Theta)$, $\Theta = diag\{1/\theta_1, ..., 1/\theta_N\}$, the protocols (43) and (46) will be constructed for finite switching states $F(t)$.

Proof: Based on Lemma 1, the matrix L_1 is invertible. Thereby, the dynamic platoon management problem will be solved if and only if both error dynamics $\tilde{\xi}_i(t)$ and $\chi_i(t)$ converge synchronously to zero. Then, consider the Lyapunov function as follows

$$
\begin{aligned}
V(\tilde{\xi}, \chi, t) = &V_1(\tilde{\xi}, t) + V_2(\tilde{\xi}, \chi, t), \\
V_1(\tilde{\xi}, t) = &8 \beta^{-1} \lambda_{\max}(T_2^\top P^{-1} T_2) \tilde{\xi}^\top(t) (\Theta \otimes P_0) \tilde{\xi}(t), \\
V_2(\tilde{\xi}, \chi, t) = &\chi^\top(t) (\Theta \otimes P^{-1}) \chi(t).
\end{aligned} \tag{59}
$$

The proof of the main results includes two parts. Part i: taking the time derivative of $V_1(\tilde{\xi}, t)$ along the trajectories of system (55) gives

$$\begin{aligned}\dot{V}_1(\tilde{\xi},t) \leq & 8\beta^{-1}\lambda_{\max}(T_2^\top P^{-1}T_2)(\tilde{\xi}^\top(t)(\Theta\otimes(P_0+P_0^\top) \\ & -2c(\Theta L_1\otimes P_0Q))\tilde{\xi}(t) \\ & -2c_0\tilde{\xi}^\top(t)(\Theta\otimes P_0)\mathrm{sgn}\left((L_1\otimes Q)\,\tilde{\xi}(t)\right) \\ & +2\tilde{\xi}^\top(t)\,(\Theta\otimes P_0)\,\breve{a}(t)).\end{aligned} \tag{60}$$

Then, we have

$$\begin{aligned}\dot{V}_1(\tilde{\xi},t) \leq & 8\beta^{-1}\lambda_{\max}(T_2^\top P^{-1}T_2)(\tilde{\xi}^\top(t)(\Theta\otimes(P_0+P_0^\top) \\ & -\omega\theta_0(\Theta\otimes P_0Q))\tilde{\xi}(t) \\ & -2c_0\tilde{\xi}^\top(t)(\Theta\otimes P_0)\mathrm{sgn}((L_1\otimes Q)\tilde{\xi}(t)) \\ & +2\tilde{\xi}^\top(t)(\Theta\otimes P_0)\breve{a}(t)).\end{aligned} \tag{61}$$

where $c > \omega/\lambda_0$, where $\lambda_0 = \lambda_{\min}(\Theta L_1 + (L_1)^\top\Theta)$, $\Theta = diag\,\{1/\theta_1,\ldots,1/\theta_N\}$, $\theta = \min\theta_i$, θ_i is defined in Lemma 1.

With $Q = T^{-1}P_0$, we have

$$\begin{aligned} & -2c_0\tilde{\xi}^\top(t)(\Theta\otimes P_0)\mathrm{sgn}\left((L_1\otimes Q)\tilde{\xi}(t)\right) \\ & +2\tilde{\xi}^\top(t)(\Theta\otimes P_0)\breve{a}(t) \\ \leq & -2c_0\tilde{\xi}^\top(t)(I_N\otimes T)(L_1\otimes P_0T^{-1})\mathrm{sgn}\left(\left(L_1\otimes T^{-1}P_0\right)\tilde{\xi}(t)\right) \\ & +2\tilde{\xi}^\top(t)(I_N\otimes T)\left(L_1\otimes P_0T^{-1}\right)\breve{a}(t) \\ \leq & -2(c_0-(1+\frac{1}{\tau})a_{\max})(I_N\otimes T)\left(\left\|\left(L_1\otimes P_0T^{-1}\right)\tilde{\xi}^\top(t)\right\|_1\right).\end{aligned} \tag{62}$$

where the last inequality is obtained by using Holder's inequality. Let $c_0 = (1+\frac{1}{\tau})a_{max}$. Then, using (57) and (62) and the Schur complement lemma, we have

$$\dot{V}_1(\tilde{\xi},t) \leq -8\beta^{-1}\tilde{\xi}^\top(t)(\Theta\otimes T_2^\top P^{-1}T_2)\tilde{\xi}(t). \tag{63}$$

Part ii: the time derivative of $V_2(\tilde{\xi},\chi,t)$ along the trajectories of the system (56) takes

$$\begin{aligned}\dot{V}_2(\tilde{\xi},\phi,t) \leq & \chi^\top(t)(\Theta\otimes P^{-1}A+\Theta\otimes A^\top P^{-1})\chi(t) \\ & -2\chi^\top(t)(\Theta L_1\otimes P^{-1}M_1)\chi(t) \\ & -2\chi^\top(t)(\Theta L_1\otimes P^{-1}M_2)\chi(t) \\ & -2\chi^\top(t)(\Theta D\otimes P^{-1}M_3)\chi(t) \\ & -2c\chi^\top(t)(\Theta L_1\otimes P^{-1}BK)\chi(t) \\ & +2\chi^\top(t)(\Theta\otimes P^{-1}T_2)\tilde{\xi}(t) \\ & +2\chi^\top(t)(\Theta\otimes P^{-1}T_2)\acute{a} \\ & -2\hat{c}\chi^\top(t)(\Theta\otimes P^{-1})\mathrm{sgn}\left((L_1\otimes BK)\,\chi(t)\right)\end{aligned} \tag{64}$$

Similarly, with $K = \kappa B^\top P^{-1}$, we have

$$\begin{aligned} & -2\hat{c}\chi^\top(t)(\Theta\otimes P^{-1})\mathrm{sgn}\left(\kappa(L_1\otimes BB^\top P^{-1})\chi(t)\right) \\ & +2\chi^\top(t)(\Theta\otimes P^{-1}T_2)\acute{a} \\ \leq & -2\hat{c}c_1\chi^\top(t)\left(\kappa(L_1\otimes P^{-1}(BB^\top)^\top)\right) \\ & \times\mathrm{sgn}\left(\kappa\big(L_1\otimes BB^\top P^{-1}\big)\,\chi(t)\right) \\ & +2c_2\chi^\top(t)\left(\kappa(L_1\otimes P^{-1}(BB^\top)^\top)\right)\acute{a}(t) \\ \leq & -2\left(\hat{c}c_1-ba_{max}c_2\right)\left(\left\|\kappa\left(L_1\otimes P^{-1}(BB^\top)^\top\right)\chi^\top(t)\right\|_1\right).\end{aligned} \tag{65}$$

where $c_1 = \lambda_{min}((BB^\top)^\top/\kappa)$, $c_2 = \lambda_{min}((BB^\top)^\top/\kappa T_2)$, and $b = 1 + \frac{\lambda_{\max}(h_{i0})}{\frac{1}{\tau}}$. Let $\hat{c}c_1 = ba_{max}c_2$. Then, we have

$$\begin{aligned}\dot{V}_2(\tilde{\xi},\phi,t) \leq & \chi^\top(t)(\Theta\otimes P^{-1}A+\Theta\otimes A^\top P^{-1})\chi(t) \\ & -2\chi^\top(t)(\Theta L_1\otimes P^{-1}M_1)\chi(t) \\ & -2\chi^\top(t)(\Theta L_1\otimes P^{-1}M_2)\chi(t) \\ & -2\chi^\top(t)(\Theta D\otimes P^{-1}M_3)\chi(t) \\ & -\omega\theta_0\kappa\chi^\top(t)(\Theta\otimes P^{-1}BB^\top P^{-1})\chi(t) \\ & +2\chi^\top(t)(\Theta\otimes P^{-1}T_2)\tilde{\xi}(t).\end{aligned} \tag{66}$$

Let $\tilde{\chi}^\top(t) = [\tilde{\chi}_1^\top(t),\ldots,\tilde{\chi}_N^\top(t)]^\top$, where $\tilde{\chi}_i^\top(t) = P^{-1}\chi_i^\top(t)$, $i = 1,\ldots,N$. It follows from (58) and (64) - (66) that

$$\begin{aligned}\dot{V}_2(\tilde{\xi},\chi,t) \leq & -\beta\chi^\top(t)(\Theta\otimes P^{-1})\chi(t) \\ & +2\chi^\top(t)(\Theta\otimes P^{-1}T_2)\tilde{\xi}(t).\end{aligned} \tag{67}$$

Thus, it follows from (59), (63) and (67) that

$$\dot{V}(\tilde{\xi},\chi,t) \leq \begin{pmatrix}\tilde{\xi}(t)\\ \chi(t)\end{pmatrix}^\top \begin{pmatrix}\Omega_{11} & \Omega_{12}\\ * & \Omega_{22}\end{pmatrix}\begin{pmatrix}\tilde{\xi}(t)\\ \chi(t)\end{pmatrix}, \tag{68}$$

where $\Omega_{11} = -8\beta^{-1}\left(\Theta\otimes T_2^\top P^{-1}T_2\right)$, $\Omega_{12} = 2\left(\Theta\otimes T_2^\top P^{-1}\right)$, and $\Omega_{22} = -\beta\left(\Theta\otimes P^{-1}\right)$. It is obtained that $\Omega_{11} < 0, \Omega_{22} < 0$ and $\Omega_{11} - \Omega_{12}\Omega_{22}^{-1}\Omega_{12}^\top = \frac{\Omega_{11}}{2} < 0$, and which is Schur equivalent to $\Omega = \begin{bmatrix}\Omega_{11} & \Omega_{12}\\ * & \Omega_{22}\end{bmatrix} < 0$. Then, it is resulting that both error dynamics $\tilde{\xi}(t)$ and $\chi(t)$ converge synchronously to the origin as $t\to\infty$. Therefore, the dynamic platoon management problem is solved by the proposed protocols (43) and (46). The proof is complete. ■

D. A finite-time convergence solution of robust cooperative trajectory tracking optimization

Although the stability analysis of Theorem 1 provides a strategy to verify the feasible design of platoon controllers under **C-V-C-VI**, the performance of the mixed traffic flow cannot be guaranteed in realistic scenarios because the strict stability of Theorem 1 relies on an infinite time horizon. To this end, we introduce the following optimization problem to guarantee that the dynamic platoon can be formulated in a finite time under a robust solution by introducing a tolerable level $\tilde{\delta}$.

$$\max \tilde{T} \tag{69}$$

$$Subject\ to:$$

$$\tilde{T} \leq \hat{T}, \tag{70}$$

$$v_0^{tra} \leq v_{\max}, \tag{71}$$

$$\tilde{T} = \frac{\ln(\tilde{\delta}^2 \lambda_{\min}(\tilde{\Omega}_1)) - \ln V(0)}{-\frac{\lambda_{\min}(\tilde{\Omega}_2)}{\lambda_{\min}(\tilde{\Omega}_1)}} \tag{72}$$

$$V(0) = \hat{\chi}(0)^\top (\Theta \otimes P^{-1}))\hat{\chi}(0), \tag{73}$$

$$\tilde{\Omega}_2 = -\Omega, \tag{74}$$

$$\tilde{\Omega}_1 = \begin{pmatrix} \Omega_1 & 0 \\ * & \Omega_2 \end{pmatrix}, \tag{75}$$

$$\Omega_1 = 8\beta^{-1}\lambda_{\max}\left(T_2^\top P^{-1} T_2\right)(\Theta \otimes P_0), \tag{76}$$

$$\Omega_2 = \left(\Theta \otimes P^{-1}\right), \tag{77}$$

$$\hat{\chi}(0) = [\hat{\chi}_1^\top(0), \ldots, \hat{\chi}_N^\top(0)]^\top, \tag{78}$$

$$\hat{\chi}_i(0) = [s_i(0) - s_0(0) + i \times (2 \times l_c) + D_{i0} + h_{i0}v_i(t), \tag{79}$$

$$v_i(0) - v_0^{tra}, a_i(0) - \xi_i(0)]^\top, \tag{80}$$

$$\tilde{\delta} > 0, \tag{81}$$

where P is derived in (58), β is a convergence rate specified in (58). Let $\tilde{T}$ be the optimal value, and v_0^{tra} is the resulting *Leader CAV*'s reference speed under the different switching states and **C-I - C-VI**. Then, the solution $\tilde{T}$ will be the final optimal time to implement the control stability.

Then, we present the following result.

Theorem 2: The robust optimization problem of the cooperative trajectory tracking can be solved if the parameters β can be properly selected such that the constraints (69) - (80) can be satisfied.

Proof: To prove our result, we first formulate the tolerant level of the platoon error $\tilde{\delta}$ as follows

$$\lim_{t \to \tilde{T}} ||(\chi(t), \tilde{\xi}(t))^\top|| \leq \tilde{\delta}. \tag{82}$$

Then, according to (68), we have

$$\dot{V}\left(\tilde{\xi}, \chi, t\right) \triangleq \Xi^\top(t)\Omega\Xi(t), \tag{83}$$

where $\Xi(t) = \begin{pmatrix} \tilde{\xi}(t) \\ \chi(t) \end{pmatrix}$. It follows from the Lyapunov function (59) that $V(t) = \Xi^\top(t)\tilde{\Omega}_1\Xi(t)$, where $\tilde{\Omega}_1 = \begin{pmatrix} \Omega_1 & 0 \\ * & \Omega_2 \end{pmatrix}$, $\Omega_1 = 8\beta^{-1}\lambda_{\max}\left(T_2^\top P^{-1} T_2\right)(\Theta \otimes P_0)$, $\Omega_2 = \left(\Theta \otimes P^{-1}\right)$. With the condition (83), we have $\dot{V}(t) \leq -\Xi^\top(t)\tilde{\Omega}_2\Xi(t)$ where $\tilde{\Omega}_2 = -\Omega$. Thus, $V(t) \leq ||\Xi(t)||^2 \lambda_{min}(\tilde{\Omega}_1) \leq V(0)e^{-\frac{\lambda_{min}(\tilde{\Omega}_2)}{\lambda_{min}(\tilde{\Omega}_1)}t}$, namely

$$||\Xi(t)|| \leq \sqrt{\frac{V(0)e^{-\frac{\lambda_{min}(\tilde{\Omega}_2)}{\lambda_{min}(\tilde{\Omega}_1)}t}}{\lambda_{min}(\tilde{\Omega}_1)}} \tag{84}$$

We choose $\tilde{T} \in \mathbb{R}^+$ such that $||\Xi(\tilde{T})|| \leq \tilde{\delta}$. Thus, we can sufficiently choose

$$\tilde{T} \geq \frac{ln(\tilde{\delta}^2 \lambda_{min}(\tilde{\Omega}_1)) - lnV(0)}{-\frac{\lambda_{min}(\tilde{\Omega}_2)}{\lambda_{min}(\tilde{\Omega}_1)}} \tag{85}$$

To ensure a quick stability, we simply choose

$$\tilde{T} = \frac{ln(\tilde{\delta}^2 \lambda_{min}(\tilde{\Omega}_1)) - lnV(0)}{-\frac{\lambda_{min}(\tilde{\Omega}_2)}{\lambda_{min}(\tilde{\Omega}_1)}} \tag{86}$$

Which is the condition (72) specified in the robust optimization problem. Then, we can select a proper convergence rate $\hat{\beta}$ to check the condition (70). The proof is completed. ∎

VI. Simulations

This section presents a series of simulation cases to demonstrate the effectiveness of the proposed cooperative driving, optimization, and automatic decision-making framework for the mixed traffic flows consisting of six *Follower CAVs* and one *Leader CAV* with the reaction-time delay and car-following dynamics, uncontrollable SCIBs of the HDVs, and realistic inter-vehicle constraints on a straight unsignalized road. Different from the existing works [9]–[12] that only consider a single lane, the dynamic platoon management in this paper will be affected by estimating the trajectories of the SVs in multiple SCIBs and calculating the unknown acceleration inputs from the connected vehicles environments in the ADMDSS. Specifically, we here formulate a finite state machine imposing the observation and prediction information to determine the driving state of the platoon under the interaction with a specific HDV, as explained in Figure 5, where all the driving conditions will be described by a function $F(t) = \{0, 1, 2, 3\}$ representing the state of the *Cruising*, *Following control*, *Real-time tracking control*, and *Avoidance in advance*, respectively. In simulations, the influence of the small differences in lateral dynamics for the platoon CAVs will be ignored in the straight lane. Besides, although the specific HDV is considered in case studies, the multiple HDVs are available by using the ADMDSS according to Algorithm 1. The vehicle parameters are shown in the following Table I.

TABLE I
DRIVING PARAMETERS

Parameters	Value	Unit	Parameters	Value	Unit
h_c	0.9	m	$v_{i,max}$	27.5	m/s
l_0	7.5	m	$v_{i,min}$	2.5	m/s
l_c	2.5	m	$a_{i,max}$	2.778	m/s^2
$\hat{\alpha}$	0.5	s^{-1}	$a_{i,min}$	-2.5	m/s^2
$\hat{\alpha}$	0.05	s^{-2}	D_1	6.75	m/s
τ	0.4	s	D_2	7.91	m/s
v_0	22	m/s	D_3	0.13	m^{-1}
v_{t_i}	24	m/s	D_4	1.59	
D_{i0}	$12.5 * i$	m	h_{i0}	$0.1 * i$	s

A. Driving scenario I: STATE 1-Cruising under F=0

In the simulation, we first consider the case that the HDV is driving at a constant speed and far away from the platoon CAVs

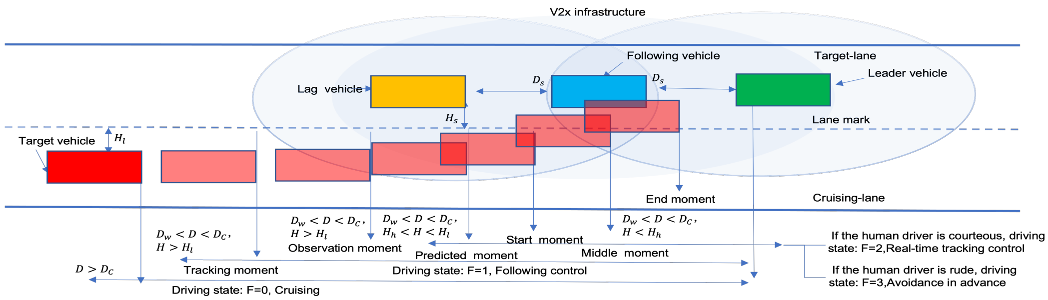

Fig. 5. Car-following environment with SCIBs.

imposing a fixed reaction-time delay and realistic inter-vehicle constraints within the start stage [0,40s] in a straight unsignalized road, where the initial velocities of the *Leader CAV* and the specific HDV are assumed as $v_0 = 22(m/s)$ and $v_{t_i} = 24(m/s)$, and the initial headway of longitudinal is large than $200m$, respectively. Notably, since we consider the car-following model and the difference velocity models in the vehicle dynamics, the proposed dynamic platoon management framework can provide the optimal speed for CAVs with an adjustable sensitivity and reflect the difference errors between the current CAV and its neighboring CAVs such that the existing the pure platoon control framework that only consider the local interaction information [11], [44] will be a special case. To start, the CAV communication is given by the matrix: $L = \begin{bmatrix} 0 & 0 & 0 & 0 & 0 & 0 & 0 \\ -1 & 1 & 0 & 0 & 0 & 0 & 0 \\ 0 & -2 & 2 & 0 & 0 & 0 & 0 \\ 0 & 0 & -4 & 4 & 0 & 0 & 0 \\ 0 & 0 & 0 & -1 & 1 & 0 & 0 \\ 0 & 0 & 0 & 0 & -1 & 1 & 0 \\ 0 & 0 & 0 & 0 & 0 & -3 & 3 \end{bmatrix}$, which can be easy to implement by C-V2X infrastructure. Let $\hat{\beta} = 1$, $\hat{\kappa} = 1$. According to the Algorithm 1 of the ADMDSS, the cruising distance satisfies $D > D_c$ such that the traveling behaviors of the platoon CAVs under **C-I** will not be affected by the HDV and the platoon CAVs will be in the *STATE 1-Cruising* so $F(t) = 0$. In addition, according to the directed communication topology condition, we get $\lambda_0 = 0.038$. With Lemma 1, we get $\theta_0 = 1$. By setting $\omega = 1$ and $\kappa = 1$, we can obtain $\alpha > \omega/\lambda_0 = 26.3158$. Then, take $\alpha = 26.4 > 26.3158$. With such conditions, it is easy to check the feasible solution of the equation (58) and the protocol (43) will be constructed under **C-V**. Then, we can show the dynamic platoon management of CAVs under the longitudinal profile. By setting the initial parameters of accelerations, the trajectories of velocity and acceleration of the CAVs systems (6) and (7) under the optimal velocity functions $y_i(t)$ and difference velocity model $g_i(t)$ can be obtained, as shown in Figs. 6. (a) and (b), respectively. Define the average space error distance and vehicle space error distance as $Error_0(t) = \frac{1}{6}\sqrt{\sum_{i=1}^{6} \|x_i(t) - x_0(t)\|^2}$ and $Error_i(t) = \sqrt{\|x_i(t) - x_0(t)\|^2}, i = 1, \ldots, 6$, respectively. Besides, define the average control energy and vehicle control energy as $Energy_0(t) = \frac{1}{6}\sqrt{\sum_{i=1}^{6} \|Energy_i(t)\|^2}$ and $Energy_i(t) = \sqrt{\|u_i(t) + y_i(t) + g_i(t)\|^2}, i = 1, \ldots, 6$, respectively. The results of Figs. 6. (c) - (d) illustrate that the proposed algorithm has achieved the dynamic platoon management of the CAVs.

B. Driving scenario II: STATE 2-Following control under F=1

With STATE 1 driving on unsignalized roads, we have known that the minimum longitudinal distance between the HDV and the *Leader CAV* will approach $120m$ which implies that the HDV will drive into the communication range of the platoon within the *observation stage*. When the HDV has a constant velocity, the platoon will be in the *STATE 2-Following control* so $F = 1$ according to the proposed Algorithm 1 of the ADMDSS. In this condition, the ADMDSS will plan a reference speed for the *Leader CAV* so that the platoon can employ the proposed cooperative driving strategy to maintain a safe distance with respect to the HDV. Similarly, we also consider the lateral velocity as zero. Then, we first plan the longitudinal reference velocity for the *Leader CAV* under **C-II**. According to the conditions (24) and (25), we get that $D_f = 14.9m$ under the parameters $\mu = 0.1$ and $D_{f0} = 12.5m$. Then, letting $\hat{\delta} = 0.02$, the planning longitudinal reference velocity of the *Leader CAV* is $24.3380m/s$. With the parameter $\zeta = 6$, we have $\delta = 0.4630m/s^2$ and $t_* = 5.0497$. Letting $\kappa = 1$ and $\beta = 6.6989$, we can obtain the solution of the optimization problem (68) as $= 5.0494s$. Therefore, the *Leader CAV* will have the acceleration $0.4630m/s^2$ at $[40, 45.0494]s$ to adjust the cruising speed from $22m/s$ to $24.3380m/s$ such that the travelling distance $D_f = 14.9m$ can be maintained with the HDV that travels with the constant speed $24m/s$. Then, we will show the dynamic platoon management of CAVs under the planning trajectory in the longitudinal profile and the protocol (46) constructed by **C-VI**. By setting the initial parameters from STATE 1 and the tolerable level $\tilde{\delta} = 0.3$, the trajectories of velocity and acceleration of the CAVs systems (6) and (7) under the optimal velocity functions $y_i(t)$ and difference velocity model $g_i(t)$ can be obtained, as shown in Figs. 7. (a) and (b), respectively. In addition, the average space error distance, the vehicle space error distance, the average control energy, and the vehicle control energy are shown in Figs. 7. (c) - (d) which implies that the dynamic platoon management of the CAVs has been achieved in a finite time.

C. Driving scenario III: STATE 3-Real-time tracking control under F=2

In this case, we assume that the HDV is courteous and has a longitudinal acceleration at $40s$ as shown in Fig. 5, which results in that the minimum longitudinal distance between the

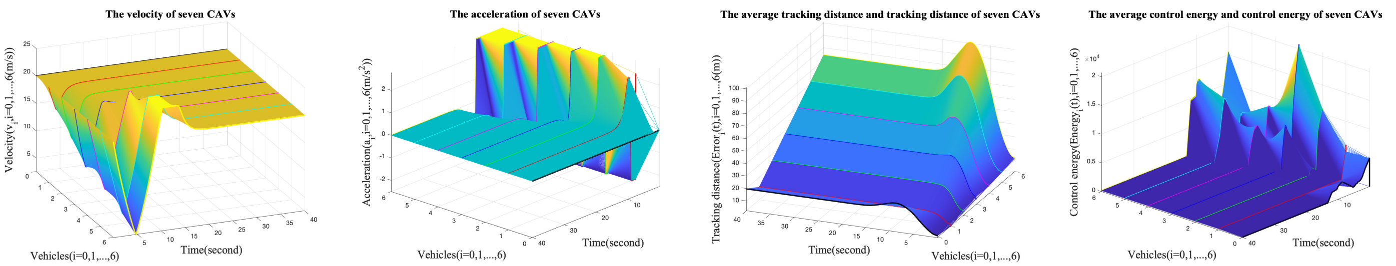

(a) The velocity of seven CAVs; (b) The acceleration of seven CAVs; (c) The average tracking distance and tracking distance of seven CAVs. (d) The average control energy and control energy of seven CAVs;

Fig. 6. Dynamic platoon management with 7 CAVs under the protocol (43) with **C-V** in the *STATE 1-Cruising*.

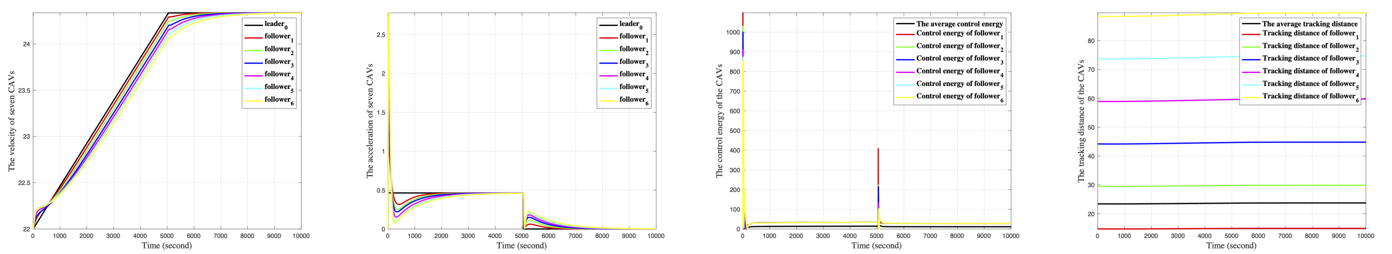

(a) The velocity of seven CAVs; (b) The acceleration of seven CAVs; (c) The average tracking distance and tracking distance of seven CAVs. (d) The average control energy and control energy of seven CAVs;

Fig. 7. Dynamic platoon management with 7 CAVs under the protocol (46) with **C-VI** in the *STATE 2-Following control*.

HDV and the *Leader CAV* will be smaller than that in STATE 2. Since the HDVs are not controllable, the HDVs may interact with the platoon CAVs with different CIIs by choosing different driving speeds in the *Tracking moment*, *Observe moment*, and *Prediction moment* to deliver the SCIIs, and the platoon will be in the *STATE 3-Real-time tracking control* so $F = 2$ according to the proposed Algorithm 1 of the ADMDSS. Therefore, the *Leader CAV* and *Lag CAV* need to observe and estimate the possible trajectory of the SCIBs of the HDVs to generate the reference trajectory planning and form the platoon in a finite time. To do this, we first consider that the longitudinal velocity of the *Leader CAV* is constant as $24.3380m/s$ in the *Tracking moment* and *observe moment* traveling on the roads, and the lateral velocity is $0.03 * cos(t)m/s$, respectively. By settings $k_i = 1, i = 1, \ldots, 6$, $a_c = 8$ and $b_c = 3$, the underlying SCIBs of the HDV will be predicted by using the social cost function (15) and the collision check condition (11) with a safe buffer field that constructed by the Ellipse with $D_b = 8$ and $H_b = 3$ being the long and short axis, the standard trajectory [45] and the predicted trajectory of the *Lag CAV*, as the blue line shown in the Fig 8. To avoid collision with respect to the predicted interaction points(black circle), the longitudinal velocities of the *Leader CAV* will be adjusted in the *Predicted moment*, i.e., the traveling distance of the *Lag CAV* should not be smaller than adjusted predicted interaction point(red star), as shown in Fig. 8. Then, the real minimum distance between the HDV and the *Lag CAV* is $27.3984m$ after $45.1s$ which can cover the states in STATE 2. Now, the automatic driving decision process for the ADMDSS is given by the following Table II, where Case 1 and Case 2 are for the different traveling conditions. Table II shows that all the over distances for the different reference trajectory plannings are larger than the longitudinal safe buffer distance $8m$ which can avoid the collision between the possible SCIBs of the HDVs and the *Lag CAV*. By setting the initial parameters from STATE 2 and the tolerable level $\tilde{\delta} = 0.3$, the trajectories of velocity and acceleration of CAVs systems (6) and (7) under the optimal velocity functions $y_i(t)$ and difference velocity model $g_i(t)$ can be obtained, as shown in Figs. 9. (a) and (b), respectively. In addition, the average space error distance, the vehicle space error distance, the average control energy, and the vehicle control energy are given in Figs. 9. (c) - (d) which implies that the dynamic platoon management of the CAVs has been achieved in a finite time to avoid collision and preferentially through the predicted interaction points.

D. Driving scenario IV: STATE 4-Real-time tracking control under F=3

We now consider that the HDV is rude and may have a CII to interact with the *Leader CAV*. The vehicle parameters and drivers' dynamics are the same as those in STATE 2 and STATE 3. By settings $k_i = 1, i = 1, \ldots, 6$, $\mu_0 = 0.18$, $a_c = 4$, and $b_c = 2$, the likely SCIBs of HDV will be predicted by using the social cost function (15), the collision check condition (11) with the defined safe buffer field, the standard trajectory [45], and the predicted trajectory of *Leader CAV*, as the blue line shown in the Fig. 10. To avoid collision with respect to the predicted interaction points(black circle), the longitudinal velocities of the *Leader CAV*

TABLE II
DRIVING PARAMETERS FOR THE AUTOMATIC DRIVING DECISION PROCESS FOR THE ADMDSS

Cases	Tracking acceleration	(Gap 5m) time	Observer moment deceleration	(Travel 5m) time	Predicted moment acceleration	Planning references CS:5s	CS:4s	Start moment CS:5s	CS:4s	Start point CS:5s	CS:4s	Over distance CS:5s	CS:4s
1	$[24 \rightarrow 25]m/s$	$169.1259s$	$[25 \rightarrow 25]m/s$	$6.0381s$	$[25 \rightarrow 25]m/s$	$25.2555m/s\&0.1835m/s^2$	$25.1988m/s\&0.2152m/s^2$	185.1381s	184.1381s	125m	100m	8.0026m	8.0010m
2	$[24 \rightarrow 25]m/s$	$169.1259s$	$[25 \rightarrow 24.3380]m/s$	$12.0761s$	$[24.3380 \rightarrow 25]m/s$	$24.8530m/s\&0.103m/s^2$	$24.8324m/s\&0.1236m/s^2$	191.1761s	190.1761s	123.3450m	98.6760m	8.0013m	8.0012m

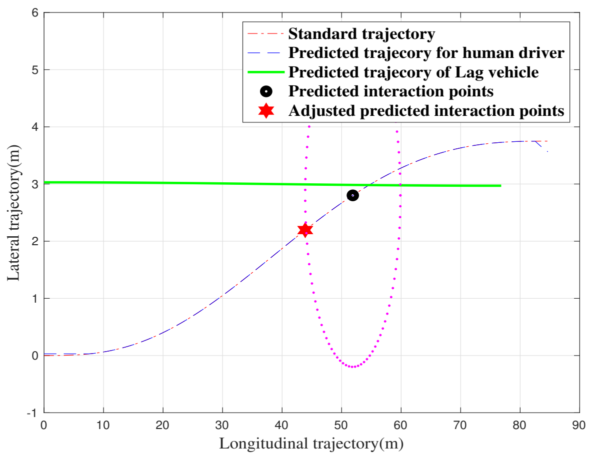

Fig. 8. Predicted trajectories and interaction points for the *Lag CAV* and the possible SICBs of the HDV using the conditions (15) and (11).

under **C-VI** will be adjusted in the *Predicted moment* to ensure that the traveling distance of the *Leader CAV* will not be larger than adjusted predicted interaction point(red star) in the roads, as shown in the Fig. 10. After $45.1s$, the real minimum distances between the possible SCIBs of the HDV and the *Leader CAV* is $117.0012m$ in the roads. We now consider the automatic driving decision process for the ADMDSS as given in the following Table III, where Case 1 and Case 2 are the traveling conditions and all the over distances are smaller than safe distance $12.5m$ to avoid the collision between the underlying SCIBs of the HDVs and the *Leader CAV*, respectively. By setting the initial parameters from STATE 2 and the tolerable level $\tilde{\delta} = 0.3$, the trajectories of velocity and acceleration of the CAVs systems (6) and (7) under the optimal velocity functions $y_i(t)$ and difference velocity model $g_i(t)$ can be obtained, as shown in Figs. 11. (a) and (b), respectively. In addition, the average space error distance, the vehicle space error distance, the average control energy, and the vehicle control energy are shown in Figs. 11. (c) - (d) which implies that the dynamic platoon management of the CAVs has been achieved in a finite time and the cruising distance of the *Leader CAV* is less than the predicted interaction point to avoid collision and the possible SCIBs of the HDVs.

VII. Conclusions

This paper addresses the problem of cooperative driving of CAVs in a mixed traffic flow consisting of multiple CAVs with the reaction-time delay and possible SCIBs of the HDVs on unsignalized roads. A novel solution strategy called ADMDSS is developed. In the proposed framework, three critical stages are established. The first one is the observation stage, in which the cruising information of all the SVs will be collected by the *Leader CAV* via C-V2X infrastructure, and then the ADMDSS is constructed to determine the driving state of the platoon. When the HDVs approach the communication range of the platoon, in the second prediction stage, the trajectory of the *Target vehicle* will be estimated and the reference trajectory planning for the *Leader CAV* and the cooperative controller for the *Follower CAVs* will be designed. While the HDVs deliver the SCIIs into the platoon, the ADMDSS will provide the high-level trajectory guidance to CAVs to adjust the time-varying inter-space error among the CAVs to prevent the possible SCIBs of the HDVs at the lane change stage and the problem of optimal energy consumption is solved in a finite time via a solution to the cooperative trajectory tracking optimization problem. Notably, the fuel economy of the platoon in this paper will be obtained by developing the optimal and economic adjusting of the *Leader CAV* which is a trade-off between driving safety and energy consumption due to the fact that the fuel consumption of the *Follower CAVs* and the *Leader CAV* are correlated as shown in simulations. In future works, we will address the influence of different regulation parameters, social cost functions, and trajectory estimation methods on platoon performance in urban roads with a specific traffic light scheme to improve the traffic throughput.

References

[1] X. Meng and C. G. Cassandras, “Trajectory optimization of autonomous agents with spatio-temporal constraints,” *IEEE Transactions on Control of Network Systems*, vol. 7, no. 3, pp. 1571–1581, 2020.

[2] ——, “Eco-driving of autonomous vehicles for nonstop crossing of signalized intersections,” *IEEE Transactions on Automation Science and Engineering*, p. inpress, 2020.

[3] G. Fitch, S. Lee, S. Klauer, J. Hankey, J. Sudweeks, and T. Dingus, “Analysis of lane-change crashes and near-crashes,” *US Department of Transportation, National Highway Traffic Safety Administration*, 2009.

[4] X. Wang, M. Yang, and D. Hurwitz, “Analysis of cut-in behavior based on naturalistic driving data,” *Accident Analysis & Prevention*, vol. 124, pp. 127–137, 2019.

[5] A. Vahidi and A. Eskandarian, “Research advances in intelligent collision avoidance and adaptive cruise control,” *IEEE Transactions on Intelligent Transportation Systems*, vol. 4, no. 3, pp. 143–153, 2003.

[6] J. Ploeg, N. Van De Wouw, and H. Nijmeijer, “Lp string stability of cascaded systems: Application to vehicle platooning,” *IEEE Transactions on Control Systems Technology*, vol. 22, no. 2, pp. 786–793, 2013.

[7] J. C. Zegers, E. Semsar-Kazerooni, J. Ploeg, N. van de Wouw, and H. Nijmeijer, “Consensus control for vehicular platooning

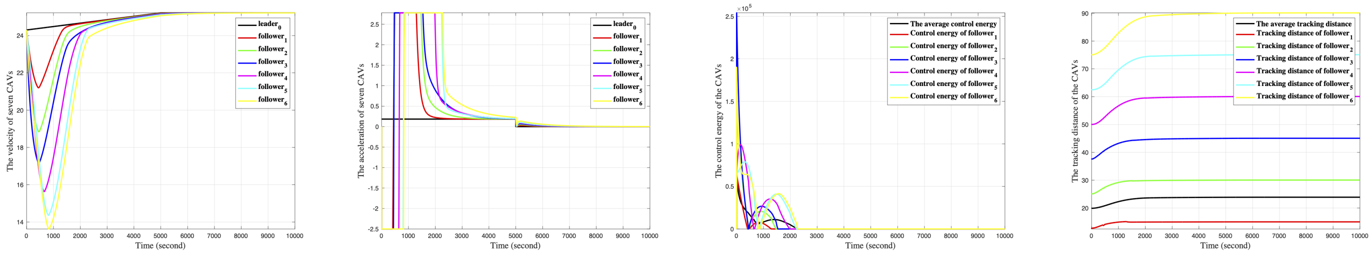

(a) The velocity of seven CAVs; (b) The acceleration of seven CAVs; (c) The average tracking distance and tracking distance of seven CAVs. (d) The average control energy and control energy of seven CAVs;

Fig. 9. Dynamic platoon management with 7 CAVs under the protocol (46) with **C-VI** in the *STATE 3-Real-time tracking control*.

TABLE III
DRIVING PARAMETERS FOR THE AUTOMATIC DRIVING DECISION PROCESS FOR THE ADMDSS

Cases	Tracking acceleration	(Gap 5m) time	Observer moment deceleration	(Travel 5m) time	Predicted moment acceleration	Planning references CS:3s	CS:2s	Start moment CS:3s	CS:2s	Start point CS:3s	CS:2s	Over distance CS:3s	CS:2s
1	$[24 \rightarrow 25]m/s$	$714.2857s$	$[25 \rightarrow 25]m/s$	$7.5529s$	$[25 \rightarrow 25]m/s$	$24.1829m/s\&-0.0517m/s^2$	$23.8728m/s\&-0.2326m/s^2$	724.8529s	723.8529s	75m	50m	12.4990m	12.4996m
2	$[24 \rightarrow 25]m/s$	$714.2857s$	$[25 \rightarrow 24]m/s$	$30.8642s$	$[24 \rightarrow 25]m/s$	$23.6627m/s\&-0.2251m/s^2$	$23.4532m/s\&-0.4424m/s^2$	748.1642s	747.1642s	73.4998m	49m	12.4995m	12.4997m

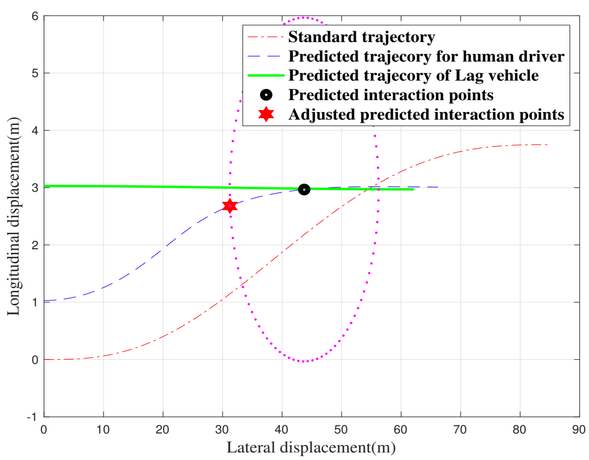

Fig. 10. Predicted trajectories and interaction points for the *Lag CAV* and the possible SCIBs of the HDV using the conditions (15) and (11).

with velocity constraints," *IEEE Transactions on Control Systems Technology*, vol. 26, no. 5, pp. 1592–1605, 2017.

[8] K. Lidström, K. Sjöberg, U. Holmberg, J. Andersson, F. Bergh, M. Bjäde, and S. Mak, "A modular cacc system integration and design," *IEEE Transactions on Intelligent Transportation Systems*, vol. 13, no. 3, pp. 1050–1061, 2012.

[9] M. Di Bernardo, A. Salvi, and S. Santini, "Distributed consensus strategy for platooning of vehicles in the presence of time-varying heterogeneous communication delays," *IEEE Transactions on Intelligent Transportation Systems*, vol. 16, no. 1, pp. 102–112, 2014.

[10] Ş. Sabău, C. Oară, S. Warnick, and A. Jadbabaie, "Optimal distributed control for platooning via sparse coprime factorizations," *IEEE Transactions on Automatic Control*, vol. 62, no. 1, pp. 305–320, 2016.

[11] S. Santini, A. Salvi, A. S. Valente, A. Pescapè, M. Segata, and R. L. Cigno, "Platooning maneuvers in vehicular networks: A distributed and consensus-based approach," *IEEE Transactions on Intelligent Vehicles*, vol. 4, no. 1, pp. 59–72, 2019.

[12] D. Zhang, Y.-P. Shen, S.-Q. Zhou, X.-W. Dong, and L. Yu, "Distributed secure platoon control of connected vehicles subject to dos attack: Theory and application," *IEEE Transactions on Systems, Man, and Cybernetics: Systems*, p. inpress, 2020.

[13] M. Bando, K. Hasebe, A. Nakayama, A. Shibata, and Y. Sugiyama, "Dynamical model of traffic congestion and numerical simulation," *Physical review E*, vol. 51, no. 2, p. 1035, 1995.

[14] D. Helbing and B. Tilch, "Generalized force model of traffic dynamics," *Physical review E*, vol. 58, no. 1, p. 133, 1998.

[15] J. Sun, Z. Zheng, and J. Sun, "Stability analysis methods and their applicability to car-following models in conventional and connected environments," *Transportation research part B: methodological*, vol. 109, pp. 212–237, 2018.

[16] B. Wang and R. Su, "Distributed observers-based cooperative platooning tracking control and optimization for connected automated vehicles with unknown jerk dynamics," *IEEE Transactions on Automatic Control*, p. under review, 2021.

[17] M. H. Basiri, B. Ghojogh, N. L. Azad, S. Fischmeister, F. Karray, and M. Crowley, "Distributed nonlinear model predictive control and metric learning for heterogeneous vehicle platooning with cut-in/cut-out maneuvers," in *2020 59th IEEE Conference on Decision and Control (CDC)*. IEEE, 2020, pp. 2849–2856.

[18] Z. Yang, Y. Feng, and H. X. Liu, "A cooperative driving framework for urban arterials in mixed traffic conditions," *Transportation research part C: emerging technologies*, vol. 124, p. 102918, 2021.

[19] N. Wu, D. Li, and Y. Xi, "Distributed integrated control of a mixed traffic network with urban and freeway networks," *IEEE Transactions on Control Systems Technology*, p. inpress, 2021.

[20] L. Wang and B. K. Horn, "On the stability analysis of mixed traffic with vehicles under car-following and bilateral control," *IEEE Transactions on Automatic Control*, vol. 65, no. 7, pp. 3076–3083, 2020.

[21] C. Chen, J. Wang, Q. Xu, J. Wang, and K. Li, "Mixed platoon control of automated and human-driven vehicles at a signalized intersection: dynamical analysis and optimal control," *Transportation Research Part C: Emerging Technologies*, vol. 127, p. 103138, 2021.

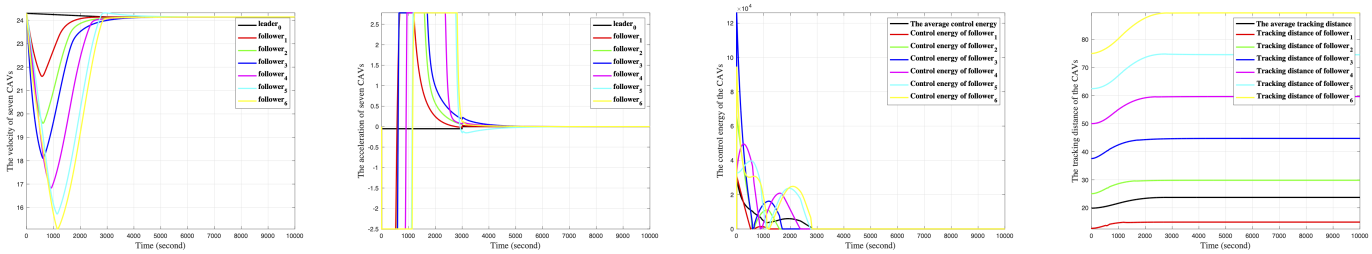

(a) The velocity of seven CAVs;

(b) The acceleration of seven CAVs;

(c) The average tracking distance and tracking distance of seven CAVs.

(d) The average control energy and control energy of seven CAVs;

Fig. 11. Dynamic platoon management with 7 CAVs under the protocol (46) with **C-VI** in the *STATE 4-Real-time tracking control*.

[22] C. Huang, H. Huang, P. Hang, H. Gao, J. Wu, Z. Huang, and C. Lv, "Personalized trajectory planning and control of lane-change maneuvers for autonomous driving," *IEEE Transactions on Vehicular Technology*, vol. 70, no. 6, pp. 5511 – 5523, 2021.

[23] Y. Liu, A. Zhou, Y. Wang, and S. Peeta, "Proactive longitudinal control to manage disruptive lane changes of human-driven vehicles in mixed-flow traffic," *IFAC-PapersOnLine*, vol. 54, no. 2, pp. 321–326, 2021.

[24] B. Asadi and A. Vahidi, "Predictive cruise control: Utilizing upcoming traffic signal information for improving fuel economy and reducing trip time," *IEEE Transactions on Control Systems Technology*, vol. 19, no. 3, pp. 707–714, 2011.

[25] H. Wang, W. Wang, S. Yuan, X. Li, and L. Sun, "On social interactions of merging behaviors at highway on-ramps in congested traffic," *arXiv preprint arXiv:2008.06156*, 2020.

[26] A. Benloucif, A.-T. Nguyen, C. Sentouh, and J.-C. Popieul, "Cooperative trajectory planning for haptic shared control between driver and automation in highway driving," *IEEE Transactions on Industrial Electronics*, vol. 66, no. 12, pp. 9846–9857, 2019.

[27] D. Invernizzi, M. Lovera, and L. Zaccarian, "Dynamic attitude planning for trajectory tracking in thrust-vectoring uavs," *IEEE Transactions on Automatic Control*, vol. 65, no. 1, pp. 453–460, 2020.

[28] S. Li, P. Durdevic, and Z. Yang, "Trajectory tracking of underactuated vtol aerial vehicles with unknown system parameters via irl," *IEEE Transactions on Automatic Control*, p. inpress, 2021.

[29] D. Tran, J. Du, W. Sheng, D. Osipychev, Y. Sun, and H. Bai, "A human-vehicle collaborative driving framework for driver assistance," *IEEE Transactions on Intelligent Transportation Systems*, vol. 20, no. 9, pp. 3470–3485, 2019.

[30] P. Hang, C. Lv, C. Huang, J. Cai, Z. Hu, and Y. Xing, "An integrated framework of decision making and motion planning for autonomous vehicles considering social behaviors," *IEEE transactions on vehicular technology*, vol. 69, no. 12, pp. 14 458–14 469, 2020.

[31] W. Wang, T. Qie, C. Yang, W. Liu, C. Xiang, and K. Huang, "An intelligent lane-changing behavior prediction and decision-making strategy for an autonomous vehicle," *IEEE Transactions on Industrial Electronics*, p. inpress, 2021.

[32] M. Treiber, A. Hennecke, and D. Helbing, "Congested traffic states in empirical observations and microscopic simulations," *Physical review E*, vol. 62, no. 2, p. 1805, 2000.

[33] L. Xiao, M. Wang, and B. Van Arem, "Realistic car-following models for microscopic simulation of adaptive and cooperative adaptive cruise control vehicles," *Transportation Research Record*, vol. 2623, no. 1, pp. 1–9, 2017.

[34] C. Flores, P. Merdrignac, R. de Charette, F. Navas, V. Milanés, and F. Nashashibi, "A cooperative car-following/emergency braking system with prediction-based pedestrian avoidance capabilities," *IEEE Transactions on Intelligent Transportation Systems*, vol. 20, no. 5, pp. 1837–1846, 2019.

[35] B. HomChaudhuri, A. Vahidi, and P. Pisu, "Fast model predictive control-based fuel efficient control strategy for a group of connected vehicles in urban road conditions," *IEEE Transactions on Control Systems Technology*, vol. 25, no. 2, pp. 760–767, 2016.

[36] Y. Liu and B. Xu, "Improved protocols and stability analysis for multivehicle cooperative autonomous systems," *IEEE Transactions on Intelligent Transportation Systems*, vol. 16, no. 5, pp. 2700–2710, 2015.

[37] S. Ammoun, F. Nashashibi, and C. Laurgeau, "An analysis of the lane changing manoeuvre on roads: the contribution of inter-vehicle cooperation via communication," in *2007 IEEE Intelligent Vehicles Symposium*. IEEE, 2007, pp. 1095–1100.

[38] E. Papadopoulos, I. Poulakakis, and I. Papadimitriou, "On path planning and obstacle avoidance for nonholonomic platforms with manipulators: A polynomial approach," *the International Journal of Robotics research*, vol. 21, no. 4, pp. 367–383, 2002.

[39] M. Werling, J. Ziegler, S. Kammel, and S. Thrun, "Optimal trajectory generation for dynamic street scenarios in a frenet frame," in *2010 IEEE International Conference on Robotics and Automation*. IEEE, 2010, pp. 987–993.

[40] Y. Chen, C. Hu, and J. Wang, "Human-centered trajectory tracking control for autonomous vehicles with driver cut-in behavior prediction," *IEEE Transactions on Vehicular Technology*, vol. 68, no. 9, pp. 8461–8471, 2019.

[41] M. Bando, K. Hasebe, K. Nakanishi, A. Nakayama, A. Shibata, and Y. Sugiyama, "Phenomenological study of dynamical model of traffic flow," *Journal de Physique I*, vol. 5, no. 11, pp. 1389–1399, 1995.

[42] M. Bando, K. Hasebe, K. Nakanishi, and A. Nakayama, "Analysis of optimal velocity model with explicit delay," *Physical Review E*, vol. 58, no. 5, p. 5429, 1998.

[43] G. Wen, Z. Duan, G. Chen, and W. Yu, "Consensus tracking of multi-agent systems with lipschitz-type node dynamics and switching topologies," *IEEE Transactions on Circuits and Systems I: Regular Papers*, vol. 61, no. 2, pp. 499–511, 2014.

[44] A. Salvi, S. Santini, and A. S. Valente, "Design, analysis and performance evaluation of a third order distributed protocol for platooning in the presence of time-varying delays and switching topologies," *Transportation Research Part C: Emerging Technologies*, vol. 80, pp. 360–383, 2017.

[45] Z. Wang, S. Cui, and T. Yu, “Automatic lane change control for intelligent connected vehicles,” in *2019 4th International Conference on Electromechanical Control Technology and Transportation (ICECTT)*. IEEE, 2019, pp. 286–289.